STRUCTURAL RESPONSE OF FLAT PLATES SUBJECTED TO TURBULENT BOUNDARY LAYER EXCITATION

A thesis paper by

SAIKAT SARKAR
ROLL NO: 001710402010
REGISTRATION NO.: 140637 OF 2017 – 2018
EXAMINATION ROLL NO.: M4CIV19015

Under the guidance of

PROF. PARTHA BHATTACHARYA

AND

PROF. ARUP GUHA NIYOGI

Submitted in partial fulfillment of the requirements for the degree of

MASTER OF ENGINEERING IN CIVIL ENGINEERING (STRUCTURAL ENGINEERING)

DEPARTMENT OF CIVIL ENGINEERING
FACULTY OF ENGINEERING AND TECHNOLOGY
JADAVPUR UNIVERSITY
KOLKATA- 700032

MAY- 2019

DEPARTMENT OF CIVIL ENGINEERING

FACULTY OF ENGINEERING AND TECHNOLOGY

JADAVPUR UNIVERSITY

KOLKATA – 700 032

CERTIFICATE OF RECOMMENDATION

This is to certify that SAIKAT SARKAR (Class Roll No.: 001710402010, Examination Roll No. M4CIV19015, Registration No.:140637of 2017 - 2018) has carried out the thesis work titled, **"STRUCTURAL RESPONSE OF FLAT PLATES SUBJECTED TO TURBULENT BOUNDARY LAYER EXCITATION",** under our direct supervision and guidance. He has carried out this work independently. We hereby recommend that the thesis be accepted in partial fulfillment of the requirements for awarding the degree of **"MASTER OF ENGINEERING IN CIVIL ENGINEERING (STRUCTURAL ENGINEERING)".**

Countersigned by

…….

Prof. Partha Bhattacharya
Professor
Department of Civil Engineering
Jadavpur University
Kolkata - 700032

…….

Prof. Arup Guha Niyogi
Professor
Department of Civil Engineering
Jadavpur University
Kolkata - 700032

……. ……..

Prof. Dipankar Chakravorty
Head of the Department
Department of Civil Engineering
Jadavpur University
Kolkata - 700032

……. ……..

Dr. Chiranjib Bhattacharjee
Dean, FET
Jadavpur University
Kolkata - 700032

DEPARTMENT OF CIVIL ENGINEERING

FACULTY OF ENGINEERING AND TECHNOLOGY

JADAVPUR UNIVERSITY

KOLKATA – 700 032

CERTIFICATE OF APPROVAL

This thesis paper is hereby approved as a credible study of an engineering subject carried out and presented in a manner satisfactorily to warrant its acceptance as a pre-requisite for the degree for which it has been submitted. It is understood that, by this approval the undersigned do not necessarily endorse or approve any statement made, opinion expressed or conclusion drawn therein, but approves the thesis paper only for the purpose for which it is submitted.

Committee of Thesis Paper Examiners

_____

Signature of Examiner

DECLARATION

I, Saikat Sarkar, Master of Engineering in Civil Engineering (Structure Engineering), Jadavpur University, Faculty of Engineering and Technology , hereby declare that the work being presented in the thesis work titled, **"STRUCTURAL RESPONSE OF FLAT PLATES SUBJECTED TO TURBULENT BOUNDARY LAYER EXCITATION",** is an authentic record of work that has been carried out in the Department of Civil Engineering, Jadavpur University, Kolkata under **Prof. PARTHA BHATTACHARYA** and **Prof. ARUP GUHA NIYOGI** Professor, Department of Civil Engineering, Jadavpur University. The work contained in this thesis has not yet been submitted in parts or full to any other university or institute or professional body for award of any degree or diploma or any fellowship.

Place: Kolkata

Date:

SAIKAT SARKAR

Roll No.: 001710402010

Registration no.: 140637

Examinations roll no. M4CIV19015

ACKNOWLEDGEMENT

I would like to express my deepest gratitude to **Prof. Partha Bhattacharya** and **Prof. Arup Guha Niyogi** Department of Civil Engineering, Jadavpur University, Kolkata-700032 for providing valuable advices, constant guidance and close supervision in all respect throughout. It is due to their regular encouragement and enlightening discussions for which this thesis has been brought to the current shape.

Very reverences to my Mother, **Late Mrs. Padma Sarkar**, Father, **Mr. Swapan Kr. Sarkar** for their support. Without their inspiration it would have been impossible.

I would also like to thank my senior lab-mate **Mr. Biplab Ranjan Adhikari** and classmates for their constant encouragement and co-operation during the preparation of this report.

Date:

…….....

SAIKAT SARKAR

Roll No: 001710402010

M.E in Civil Engineering

Jadavpur University

Kolkata- 700032

ABSTRACT

Turbulence induced structural vibration and subsequent noise generation has been a field of interest especially in aircraft and automobile industries, where passenger comfort is of major concern. The problem gets worse for structures made of lightweight panels due to excessive vibration, fatigue and resulting noise into the interior cabin. In case of high-speed moving vehicles, structures are excited by the pressure fluctuations due to the turbulent flow around the vehicles induced by their movement. This turbulent boundary layer (TBL) induced structural excitation is one of the major causes of radiated and/or transmitted noise. In order to reduce the noise level without adding extra mass to the structure, it is important to understand the mechanism of structural response due to TBL induced excitation and subsequent noise generation. Investigations have been carried out to study the behavior of the velocity and pressure fluctuations within TBL flow. Also, some empirical and semi-empirical models of wall pressure auto-spectrum under zero pressure gradient TBL flow have been proposed earlier. The present work aims to study the TBL induced structural response of a flat plate, using established empirical models and for different Mach numbers. In this study the response of a rectangular steel plate with three different boundary conditions is investigated and compared for different Mach numbers. Empirical models are used to estimate pressure spectrum. Finite Element based ANSYS (ver. 19.0 R1 (Academic)) package is used to calculate the free vibration parameters of the plate. An in-house MATLAB (ver. 2013b) code is developed to prepare frequency response function (FRF) of the plate structure, and finally another MATLAB code is developed to couple the pressure cross-power spectra and FRF for estimating the structural response. A parametric study is conducted to understand the effect of Mach number on TBL induced structural vibration, and it is observed that there is significant variation in structural response due to the change of flow parameter, namely, Mach number and structural parameters, such as, boundary conditions. Also, it is observed that the response prediction using different TBL models differs significantly in the 0 – 500 Hz frequency regime.

Keywords: Structural vibration, TBL excitation, noise radiation, FE modeling

TABLE OF CONTENTS

LIST OF SYMBOLS

SYMBOLS	NAME	SYMBOLS	NAME
$\overline{p^2}$	Mean-square pressure	u′	Fluctuation velocity
Φ	Power spectral density	u*	Time averaged velocity
ω	Angular velocity	u^+	Momentum thickness
δ	Boundary layer thickness	y^+	Normal spatial surface coordinate
δ*	Boundary layer displacement thickness	$S_{xx}(\omega)$	Auto-power spectral density
Θ	Boundary layer momentum thickness	$S_{xy}(\omega)$	Cross-power spectral density
ν	Kinematic viscosity	$\phi_{pp}(\omega)$	Single-point power Spectrum
μ	Dynamic viscosity	G_{uu}	Displacement response cross-power spectral density
ρ	Density	Γ	Coherence function
τ_ω	Wall-shear stress	ξ_1, ξ_2	Separation vectors
U_∞	Free-stream velocity	U_c	Convective velocity
U_τ	Shear velocity	ω_n	Natural angular frequency
S_h	Strouhal numbers	ω	Angular frequency
R_e or $R_{e\delta}$	Reynold number	ξ	Damping ratio
M	Mach number	φ^T	Mode shape data
x	Distance from inlet (m)	$R_{e\theta}$	Momentum Reynolds number
U_e	Velocity at the boundary-layer edge	R_T	Ratio of timescales
U	Instantaneous velocity	H	Frequency response function

LIST OF FIGURES

FIGURE No.	FIGURE NAME	PAGE No.

LIST OF TABLES

Chapter – 1

Introduction

1.1. INTRODUCTION

When air flows over a surface it appears to adhere to it, so much so that the velocity of the air stream, microscopically, is zero at the surface which is known as no-slip condition. The velocity of the flow goes increasing from zero to free stream velocity along the vertical direction from the plate surface. This thin layer which exists near the wall is called boundary layer. This concept was introduced by Ludwig Prandtl in 1904. He discovered that within the thin boundary layer the viscous effects, no matter how small the viscosity of the fluid might be, have equal importance as inertial effects. Due to friction between the air and the surface, the movement of air is slower near the surface. The relative velocity of the airflow increases rapidly with distance, away from the surface.

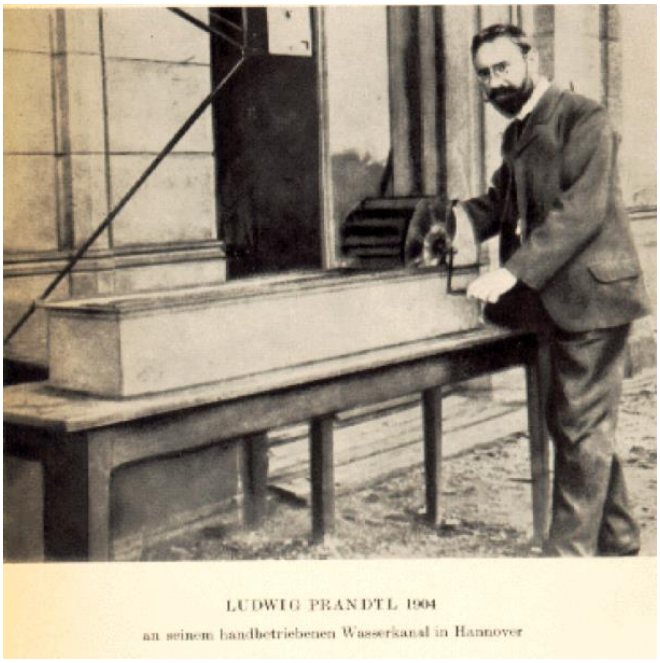

Fig. 1.1: Photograph of Prof. Ludwig Prandtl (1875-1953)[1]

A very thin boundary layer grows in the vicinity of the solid surface due to the presence of a surface. Major reason for the development of boundary layer is viscosity of the fluid. The term 'viscous' simply refers to the resistance of a fluid to shear forces, hence its resistance to physical 'flow'. A typical velocity profile is shown in Fig. 1.2 (a). The velocity is zero at the surface of the plate and at the edge of the boundary layer the velocity is approximately 99% of the free stream velocity. The adhered fluid layer can be divided into two unequal regions. One of them is outer region where the effect of viscosity is neglected. The second one is the very thin

[1] Lecture Notes in Applied Mathematics, Boundary layer in fluid dynamics, A.E.P. Veldman, University of Groningen, Netherlands, Academic year 2011-2012

boundary layer where the viscosity effect is considered. The boundary layer does not have any precise edge; the influence simply fades, depending on the viscosity of the medium, the speeds involved and the surface roughness. However, for the purpose of calculations it is necessary to define an edge. The thickness of the boundary layer increases from upstream (U/S) to the downstream (D/S) direction. However, it is clear that the thickness of a boundary layer can be determined by using the viscosity of the fluid, velocity of the flow and distance from the edge of the plate.

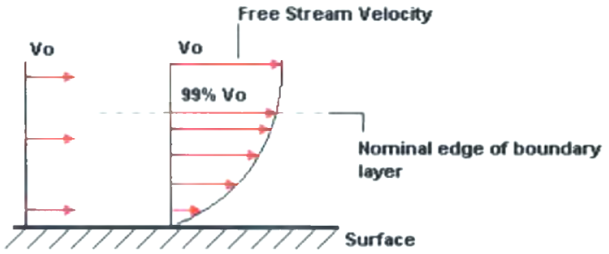

Fig. 1.2 (a): **Development and variation of velocity within the boundary layer on a flat surface with no stream line pressure variation**

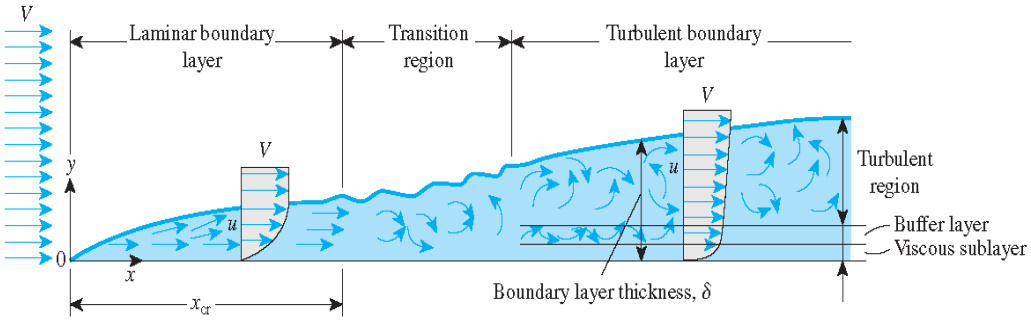

Fig. 1.2 (b): Development of the boundary layer

When a fluid flows over a solid surface it is initially laminar but it could gradually get turbulent. In the laminar flow the fluid flows over the surface in a precise and ordered fashion. The fluid molecules moves smoothly over each other within the layers but it gradually gets faster further away from surface until it reaches free stream speed. As the flow velocity increases further away from the surface, this highly-ordered condition does not last, hence any small disturbance causes a chain reaction which rapidly degenerate the order. The stream lines do not remain parallel to each other, as the fluid molecules move in a random manner. So it is difficult to predict their path. That means the entire flow structure breaks down. This situation is often referred as the turbulent boundary layer (TBL). These two types of flow have different properties. When fluid flows in the boundary layer the velocity decreases due to the viscous effect. As a result there is a losses in kinetic energy observed. A time came when flows occur in reverse direction because no energy left to push the flow in forward direction. This reverse flow is the major reason of eddy formation. The formation of eddies is the major reason of surface pressure fluctuation. Thus it

becomes necessary to identify the turbulent boundary layer. A common method of defining the type of flow is by measuring the Reynolds Number (Re) or $(R_{e\delta})$. Reynolds number is defined as the ratio of the inertia and viscous forces. It may be defined generally as,

$$\mathrm{Re} = \frac{\rho U x}{\mu} = \left(\frac{\text{Inertia Force}}{\text{Viscous Force}}\right) \tag{1.1}$$

Where,

U is the velocity (m/s),

x is the distance from inlet (m),

ρ is the density (kg/m^3)

and μ is the dynamic viscosity (kg/ms)

Up to approximately $R_e = 5 \times 10^5$, the flow is considered to be laminar and for turbulent flow the Reynolds number is taken greater than 2×10^6. The change of state of the flow from laminar to turbulent does not generally take place at a single well-defined point, but instead occurs gradually, thus creating the transition region between the two flow regimes.

Due to this surface pressure fluctuation in the TBL, the structure is subjected to random excitation. If one such structure forms a part of an enclosed chamber, the enclosed air of air tight chamber is also coupled with the vibration, resulting in generation noise.

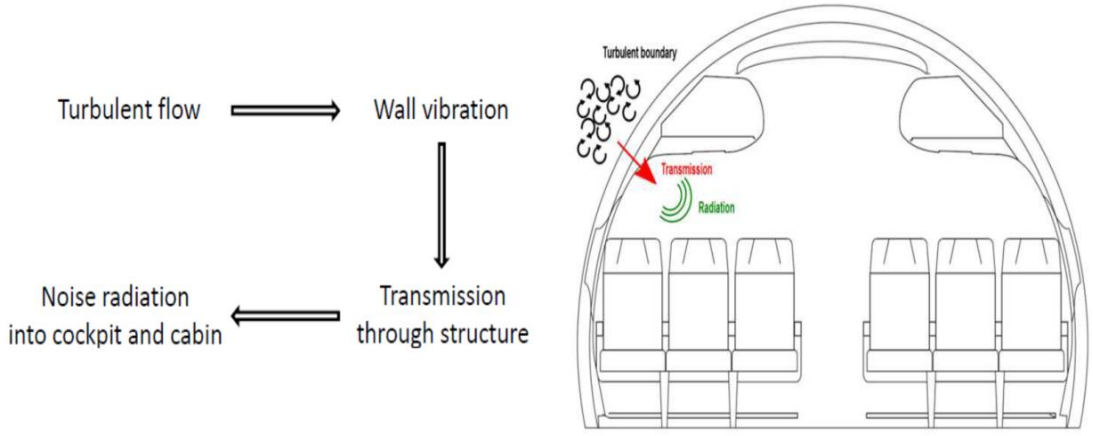

Fig. 1.3: Flow-generated-noise Mechanism [2]

The structural response due to turbulence and the radiation of sound by vibrating structure have been a topic of investigation by many authors. The random pressure fluctuation within the TBL which is the major reason of structural vibration may lead to structural fatigue and noise generation. This is the major source of noise

[2] Ref: Miloud Alaoui, Coherent structures and wall-pressure fluctuations in turbulent boundary layer subjected to pressure gradients.

generation. This fatigue and the structural vibration are the major part of the research for the past few years.

Airplanes, trains and submarines are all composed of stiffened structures that are excited by pressure fluctuations due to the turbulent flow induced by their movement. In order to reduce the noise radiated from these structures, it is important to understand turbulent boundary layer phenomenon and how a stiffened structure reacts to TBL excitation. For quite some time in aircraft industry the noise and vibration issue is gaining significant focus to make the vehicle comfortable. The increased interior noise level needs proper understanding to control noise level down to an acceptable limit and passenger comfort without affecting the weight. In past decades, many researchers have employed a simple flat panel model to theoretically explore the response of fuselage structures due to TBL pressure. It may be a good simplification for the substructure of the fuselage but not appropriate for the entire structure since it neglects the effect of the fuselage curvature. From this point of view, the cylindrical shell structure would be more acceptable in the theoretical analysis on the vibro-acoustics of fuselage-like structures subjected to the TBL pressure. In general, it was seen that the interior noise generated by TBL source is important at mid and high frequencies, and it dominates the interior noise field at frequencies that are in the range of 400 to 2000 Hz.

A large number of investigations are being done on the behavior of the velocity and pressure fluctuations within TBL flow. A large volume of researches have been conducted under zero pressure gradients over flat plates or inside the cylindrical pipe or channel. Also some empirical and semi-empirical models of wall pressure auto-spectrum under zero pressure gradient TBL flow have been conducted. In the last few decades due to progress in high-speed computers, computational fluid dynamics (CFD) has been routinely used to calculate the pressure fluctuations due to TBL. There are three different approaches for solving the equations of fluid dynamics involving turbulent flows:

(i) Reynolds-Averaged Navier-Stokes (RANS)
(ii) Large eddy simulation (LES)
(iii) Direct numerical simulation (DNS).

Some authors have worked on turbulent boundary layers subjected to zero, non-zero and canonical zero pressure gradient flow. In majority of the research, focus has been on adverse pressure flows as this type of pressure gradient can be critical in several engineering applications. One of them is separation of turbulent boundary layer over the wing when the critical angle of attack is reached.

The ultimate focus is on the noise radiation into the cabin of an aircraft or a submarine. Hence, a clear concept is needed about the noise radiation. The interior noise in an aircraft can be classified according to two transmission path: airborne and structure borne. The former includes the propagation of engine vibration through the fuselage that then radiating sound into the cabin. Also, the air-conditioning systems and the flow-induced noise due to turbulent wall pressure fluctuations imparted over

the fuselage contribute to the airborne noise. The light structure of aircraft could entrance the noise pressure level in the cabin.

Disturbances due to vibration of engine and AC duct are predictable, whereas, the excitation due to TBL is extremely random, both in frequency and spatial domains. The analysis of aircraft interior noise due to TBL excitation as practiced depends on architectural acoustics methods extrapolated from previous design and performance of aircraft. Several theoretical, numerical and experimental studies are performed to explore the vibration and radiation of sound from panels, excited by the turbulent flows. The knowledge obtained from the investigations is the power spectrum and space-time correlation of the TBL pressure fluctuation as well as the displacement and acceleration spectra of the vibrating plate. Some experimental studies are also being performed by NASA taking into consideration the aircraft interior noise induced by the TBL. These studies make few experimental data available for interior sound pressure level and skin vibrations spectra, at various locations in the cabin. Several different approaches have been applied to the analytical modeling of airborne and structure borne noise transmission into airplanes. The application of a particular method is restricted to a specific frequency range. The main methods are finite element analysis (FEA), statistical energy analysis (SEA), dynamic element analysis (DEA), and boundary element analysis (BEA).

It is indicated that the noise levels increase with Mach number. All sophisticated analysis techniques, such as SEA and DEA, use a TBL model that consists of both single-point wall pressure spectrum model and wavenumber-frequency spectrum model. The single-point wall pressure spectrum gives the frequency distribution at each point whereas, the wavenumber-frequency spectrum model allows for modal analysis.

More recent works have concentrated on conducting computational fluid dynamic simulations. Generally it is sufficiently complex to develop a complete analytical or numerical solution for flow field of a turbulent boundary layer over a complicated surface. Therefore, current TBL models continue to be developed using a combination of analytical, numerical and experimental techniques.

It is from this perspective the objective of the present work is formulated. It is proposed that the focus of the present work will be towards understanding the effect of flow behavior over the plate like structure and its consequences on the vibration response behavior on the same. Different parameter e.g. flow velocity, boundary condition etc. will varied to estimate their effect on structural vibration.

1.2. ORGANIZATION OF DISSERTATION

In Chapter 1, an introduction to the TBL, surface pressure fluctuation, TBL induced excitation and noise generation are discussed. Several types of models, which have already been applied by different investigators, are also discussed.

A detailed review of literature on this topic and the objective of the present work is presented in the *Chapter 2*.

Chapter 3 deals with the mathematical basis to fulfill the objective of the work, is presented. Firstly, the terms related to turbulent boundary layer and frequency response function is introduced. Then the turbulent flow statistics is discussed. The single-point wall-pressure spectrum model is discussed. A coherence function that estimates cross-power spectrum is also explained. Finally, the coupling of average cross-power spectrum with frequency response function to obtain structural response is described.

In Chapter 4, the detailed description of the plate geometry and boundary conditions, structural parameters and flow parameters considered, in present work and results obtained are summarized.

In the last chapter, conclusion and scope of future work is presented.

Chapter – 2

Literature Review

2. LITERATURE REVIEW

2.1. INTRODUCTION

Over the last few decades pressure fluctuations in association with turbulent boundary layer (TBL) has been an interesting issue to the investigator. To understand the noise generation and structural vibration, it is important to understand the behavior of the pressure fluctuation due to TBL. Therefore, many researchers have performed extensive experimental and computational investigations in this field. Due to huge development in computational facility, computational fluid dynamics (CFD) has been practiced by large numbers of investigators since last few years. These numerical and experimental works are also reviewed in this chapter. The three TBL models generally used as reported in existing literature are *mean-square pressure models*, *single-point wall-pressure spectrum* and the *normalized wavenumber-frequency spectrum*. The Mean-square pressure is a measure of the total energy due to TBL pressure fluctuation whereas single-point wall pressure spectrum sorts the energy into frequencies and normalized wavenumber-frequency spectrum sorts the energy into wavenumbers. These models are discussed in separate sections.

2.2. EMPIRICAL MODELS

2.2.1. MEAN-SQUARE PRESSURE FLUCTUATION MODELS

The mean square pressure is basically the time average of total energy due to TBL at a single point. In this model the field is considered as homogeneous and stationary, hence, the energy at a single point is considered. The mean square pressure fluctuation can be written as

$$\overline{p^2} = \int_0^\infty \phi(\omega) d\omega \tag{2.1}$$

where, ϕ is the Power spectral density of surface pressure fluctuation (single-sided). Several researchers, who conducted experiments to obtain mean-square pressure, took the raw time signal, squared it and averaged over time as,

$$\overline{p^2} = \frac{1}{T}\int_0^T p^2(t) dt \tag{2.2}$$

The mean-square pressure fluctuation estimation was proposed by Kraichnan [1] as a function of wall shear stress for low to moderate Mach numbers. The approximate dependence of the mean-square intensity, spatial scale, and frequency scale on Mach number, and, distance from transition point are estimated. The wave number spectrum of the pressure fluctuation distribution over the surface of the plate is expressed in terms of transforms of two-point velocity correlations and expressions are derived for the driving force exerted on a rectangular piston set in the surface of the plate. He found that the integral over the boundary surface of the two-point

quadratic correlation function of the pressure fluctuation should vanish, with the result that the mean-square force per unit area exerted on a large area of the surface should tends to zero as the area increases indefinitely. An idealized model of TBL flow was constructed by him and used to relate the spectrum and correlation function of the surface pressure distribution to the corresponding functions for a homogeneous turbulent flow.

After few years in 1960, Lilley and Hodgson [2] conducted a wind tunnel test and estimated the mean square wall pressure fluctuation as a function of dynamic pressure. Lilley and Hodgson, with a different mathematical approach, arrived at a frequency spectrum for a zero-pressure-gradient boundary layer. Willmarth and Wooldridge [3] carried out an experimental study by using a pressure transducer flush with the surface to measure the mean-square wall pressure at 150 ft/s and 200 ft/s wind velocity over a non-dimensional frequency band of $0.14 < \omega\delta^*/U_\infty < 28$. They studied the wall pressure fluctuation and the structure and scale of eddies that produce the pressure fluctuations. Their results showed that in a fully turbulent tube flow, low-frequency pressure fluctuations had the highest convection speed. They also found that the transverse and longitudinal scales of small and large-scale wall-pressure fluctuations were approximately the same. They found that the convection speed of the pressure producing eddies varied from 0.56 to 0.83 times the free stream velocity. This range for convective velocity is still used in analysis today.

Corcos [4, 5] measured the mean-square wall pressure by considering the pressure field stationary and homogenous. Basically he used the previous model of Willmarth and Wooldridge in his own experiments. He suggested a relationship for mean-square wall pressure as a function of wall shear stress, for Reynolds number of $\delta U_\infty/\nu \cong 300{,}000$ and he [4] concluded that the dependence on Reynolds number is small. He found the effect of transducer size in measurements and concluded that the transducer size is a major cause of some undesirable large errors.

Ffowcs-Williams [6] first studied the effect of compressibility which were not considered in previous work. It was revealed that the intensity of the turbulence induced surface pressure varied slowly as a function of Mach number. This study shows that the correlation area is proportional to the square of mean flow.

Bull [7] observed that mean-square wall pressure value increased with Reynolds number and it is a function of wall shear stress. He showed that the bandwidth was determined by the response characteristics of the microphone system. He was the first to discuss that the different parts of boundary layer could produce different wall pressure fluctuation frequencies. This experiment was conducted with pinhole microphones of capacity 80 to 100,000 Hz.

Lowson [8] estimated the mean-square wall pressure as a function of Mach number that can be found using the dynamic pressure. He observed the effect of pressure transducer size on the accuracy of the wall-pressure beneath a turbulent boundary layer.

Blake [9] conducted an experiment which was performed in the subsonic low-turbulence acoustic wind tunnel in the Acoustics and Vibration Laboratory at Massachuestts Institute of Technology. Smooth as well as rough wall test panels were used by him. He was the first who used very small flush mounted microphones. The smooth test panel was built from formica-coated plywood and the rough panels were prepared by mounting sand grains to unfinished plywood using shellac as adhesive. He noted that previous experimental studies were limited to the finite size of microphones and by extraneous tunnel disturbances. So, Blake conducted an experiment in a low-noise wind tunnel facility with microphones capable of better resolution. Due to improved resolution of the microphone, the constants of these relationships were higher than earlier results. He developed two relationships. One of them was based on the dynamic pressure and the second on wall shear stress.

Schewe [10] used various sizes of transducers and conducted modern wind-tunnel measurements with a flow speed of 6.3 m/s. He found the mean-square wall-pressure value as function of dynamic pressure. He pointed out that the ratio between the pressure transducer size and smallest important length-scale of the flow should be as small as possible.

Lauchle and Daniels [11] conducted a test and studied wall pressure fluctuation due to TBL for a flow of glycerin in a long pipe and found a mean-square wall pressure value. Farabee and Casarella [12] also noted that the deviation of wall-pressure for various investigators depended on the size of transducers and the Reynolds number. They obtained the value of mean-wall pressure fluctuation by numerically integrating the spectrum from 50 to 20,000 Hz. They chose the lower frequency limit at 50 Hz because the experimental facility related noise dominates below 50 Hz. They obtained a relationship dependent on the Reynolds number for $(U_\tau \delta/\nu)$.

Lueptow [13] investigated measurement effects and the turbulent wall-pressure spectrum. He developed the mean-square pressure fluctuation value as a function of the dynamic pressure. According to Farabee and Casarella mean-square pressure was dependent on the Reynolds number, but Lueptow felt that non-dimensionalizing it with dynamic pressure seemed to reduce the sensitivity to Reynolds number.

While comparing the empirical models to the experimental data for a range of Mach numbers it was seen that the Kraichnan [1] and Lueptow [13] are at the higher side of the predictions where Bull [7] and Willmarth and Wooldridge [3] are at the lower end. Farabee and Casarella [12] model is in middle of the above two predictions. The results of Lowson [8] and Corcos [4] [5] model are approximately same and similarly the prediction of Farabee and Casarella [12] and Blake [9] are in the same range.

2.2.2. SINGLE-POINT WALL-PRESSURE SPECTRUM MODELS

Robertson [14] proposed a model which is based on Lowson's model [8]. He compared Lowson's formula with the data especially measured at supersonic speeds at NASA Ames Research center. He noticed that the model proposed by Lowson underestimates the spectral levels at low Strouhal numbers ($S_h = \omega\delta / U\tau$) and gives too large a roll off at high Strouhal numbers. Therefore, he proposed a new formula that appears to be more representative of experimental findings throughout the Mach number range.

Efimtsov [15, 16] gives two single-point wall-pressure spectrum models on which the first model is referred as first model of Efimtsov or Efimtsov [15] and the second one is referred as second model of Efimtsov or Efimtsov 2 [16]. Efimtsov stated that a single-point wall-pressure spectrum model should be dependent on Mach number (M), Reynolds number (R_e), and Strouhal number (S_h). Efimtsov collected a series of flight test data in the range of Mach numbers of M = 0.41 to 2.1 with Reynolds number of $Re_x = 0.5 \times 10^8$ to 4.85×10^8. The pressure fluctuations were measured at various zones along the fuselage. Efimtsov 2 is an updated model in which the principal independent variables are the Strouhal number and the Reynolds number.

Howe [17] proposed a model and attributed it to Chase [18]. This model is a simplification of the previous model developed by Chase [18], which was more comprehensive for the wavevector-frequency spectrum. The model spectrum is proportional to ω^2 at low frequencies and varies as ω^{-1} at higher frequencies but it does not include a ω^{-5} spectral decay which has been measured and theoretically shown to exist at the highest frequencies.

In the year 2000, Smol'yakov [19, 20] found that the single-point wall-pressure spectrum scales on different variables, depending on the frequency. He described three regions as low frequency, universal and high frequency. The equations were derived in such a way that the first part of equation describes the main laws governing the behavior of the spectra and the second part provided a smooth matching between the three regions.

Goody [21] proposed an empirical model of the single-point wall-pressure spectrum beneath a two-dimensional, zero-pressure-gradient boundary layer which was based on the experimental surface pressure spectra measured by seven research groups. Goody compared the Chase-Howe [18] model to different experimental spectra that covered a range of Reynolds numbers 1.4×10^3 to 2.34×10^4. He found that the Chase-Howe [18] model was low at low frequency but did not decay rapidly enough at high frequencies. So, he modified their model by introducing a term in denominator to decay the spectral level as ω^{-5} and a constant was also multiplied in the numerator to raise the spectral levels at all frequencies to get better agreement with the experimental data.

Rackl and Weston [22] compared the measured flight data to the predictions from the second model of Efimtsov [16] single point wall pressure spectrum model and found that the Efimtsov [16] model did not predict broadband peak near a Strouhal number of 0.6. They suggested that one might expect that certain frequency regions would contribute more strongly to turbulence energies according to the length scales imposed on the flow by the boundary layer thickness.

An empirical model to predict the wall-pressure fluctuation spectra beneath adverse pressure gradient flows is presented by Rozenbeng and Robert [23]. It is based on Goody's model, which already incorporates the effect of Reynolds number but is limited to zero pressure gradient flows. The extension relies on six test cases from five experimental or numerical studies covering a large range of Reynolds number, $5.6 \times 10^2 < Re < 1.72 \times 10^4$, in both internal (channel) and external (airfoil) flows.

The Efimtsov 1 [15], Goody [21] and Smol'yakov [19, 20] models are approximately within the expected range while Chase-Howe [18] under predict and Efimtsov 2 [16] predicts over. Overall Goody's [21] single-point wall-pressure spectrum model is the most appropriate for aircraft applications.

2.2.3. NORMALIZED WAVE-NUMBER MODELS

To define the wavelength distributions, the normalized wavenumber-frequency spectrum models are used by acoustic analysis programs. In these models it is important that the normalized wavenumber-frequency model can be easily transformed from the wavenumber-frequency domain to the space-time domain. Several researchers developed different models namely Corcos [24], Mellen [25, 26], and Chase [18] etc. By reviewing those literatures it is clear that the Corcos [4, 5] model predict over results than the other models.

2.3. COMPUTATIONAL FLUID DYNAMICS (CFD) TO ESTIMATE WALL-PRESSURE FLUCTUATIONS

As 'turbulence' is an open challenge in classical physics, its prediction in any form is appreciable. Researchers have used different methods and models to estimate TBL induced pressure fluctuation. Some popular empirical and semi-empirical models, as discussed earlier, are deployed to estimate the pressure fluctuation. But, estimation of averaged flow quantities using empirical or sophisticated statistical modeling to obtain wall-pressure spectra and spatial correlation has serious limitation in case of complex flow or geometry. Favorable or adverse pressure gradients or detached flows can be considered as examples of such problem. Time dependent flow simulation is necessary to overcome this draw back. For relatively high Mach numbers, minor acoustic (compressible) contribution can also be found apart from hydrodynamic part. To accommodate the acoustic components high-fidelity compressible simulations are to be performed. Since, as the present work is focused on structural acoustics, this part of flow-acoustics is not explored.

With the exponential development of computing facilities CFD is now being widely used in industry and academia. Generally, the CFD models can be classified in three broad categories.

i) Reynolds Averaged Navier Stokes (RANS) models: RANS is popular because of its simplification to the Navier-Stokes equations. These models can efficiently estimate the time-averaged global flow quantities, i.e., RANS equations of a fluid flow motion are time averaged approximations of Navier-Stokes equations. This idea came from Reynolds decomposition, where the instantaneous properties of flow are decomposed into a mean component and a fluctuating component. But, cannot capture the fluctuating quantities at their local levels.

$$u = u^* + u' \tag{2.3}$$

Here u is the instantaneous velocity, u* is the time averaged velocity and u′ is the fluctuation velocity. The mean of the fluctuation component is zero. With the aid of this decomposition; the incompressible Navier-Stokes equation can be transformed in the time-averaged equations.

ii) Large Eddy Simulation (LES) models: LES was formulated in the late 1960s and it is more accurate than RANS for acoustic and flow separation problems. These models resolve the large eddies up to a scale which is nearly equal to the grid size, and model eddies of smaller length scales. These models can estimate the fluctuating quantities up to a length scale, which is considered to contain major portion of the total energy. Therefore, these models can be treated as a good approximation of turbulence phenomenon in real life flow problems. This method has a considerable computational cost (lower than the Direct Numerical Simulation). For that reason, a CFD model was used in order to reduce the cost due to physical and time resource limitations.

iii) Direct Numerical Simulation (DNS): In DNS, Navier-Stokes equations are numerically solved without any turbulence model. It means that both time scales and the spatial scales must be resolved without using any model. Hence, this is the most robust and computationally demanding approach, as here unsteady Navier-Stokes equations are solved at each and every node. Thereof, this method is the most reliable one, but yet the cost of computation is very high.

In his ground breaking work in 1988 Spalart [27] numerically simulated (used DNS) turbulent boundary layer on a flat plate, with zero pressure gradient at four stations between momentum thickness Reynolds number, $R_\theta = 225$ and $R_\theta = 1410$. He used 10^7 grid points to solve three-dimensional transient Navier-Stokes equations using spectral method. He applied multiple-scale approximation, in which actually some set of equations are solved with periodic conditions in the stream-wise direction providing a good approximation of the local state of boundary layer that has a slow spatial development.

Since the large-eddy simulation (LES) of wall-bounded flows are very much expensive at high Reynolds numbers, especially if dynamically important small near wall vortices are to be resolved, Wang [28] developed a numerical scheme using combination of large eddy simulation (LES) with wall modeling for simulation of wall bounded flows. This cost-effective method predicted low-order velocity statistics in good agreement with LES results.

Xiaohua *et. al.* [29] simulated turbulent boundary layer in a nominally zero-pressure-gradient smooth flat-plate for a continuous momentum thickness Reynolds number range of $80 \leq Re_\theta \leq 940$. Blasius boundary layer is maintained in the range of$80 < Re_\theta < 180$ that is early transition region with maximum 1% error in skin friction calculation. Mean and second-order turbulence statistics are compared with experimental data, which essentially constitute DNS dataset for the spatially developing boundary layer. The calculations indicate a quite high overestimation of wall shear stress in the near wall zone for the late transition region. They produced vivid evidence of hairpin vortices formation as result of the direct solution of Navier Stokes equations.

Bert and Peter [30] studied aerodynamically different cyclist positions and did CFD analysis and they put a full scale model in the wind tunnel. Three different cyclist positions were evaluated with the help of Computational Fluid dynamics (CFD) to provide reliable data and to check the accuracy of the CFD simulations. He concluded that accuracy of CFD is good when compared to wind tunnel tests.

In the PhD thesis Mahmoudnejad [31] developed higher order DNS scheme and reported about numerical investigation using four different turbulence models to calculate real time pressure and velocity fluctuations. These are as follows:

i) Direct Numerical Simulation (DNS)
ii) Proposed DNS scheme with hybrid of sixth-order weighted compact scheme (WCS).
iii) Weighted essentially non-oscillatory (WENO)
iv) Modified WENO-WCS scheme (MWWS)

She first estimated single point pressure and velocity fluctuations using different schemes stated above and a three dimensional (3D) numerical domain. Subsequently, obtained wall-pressure spectra and compared the numerical estimation with the results of existing empirical/semi-empirical models. In low frequency region, results obtained by Delayed Detached-Eddy Simulation based on Spalart-Allmaras (DDES-SA) turbulence models and MWWS scheme showed good agreement with Goody model. RANS-SA, RANS-SST and DDES-SST turbulence models showed agreement with the Robertson model. In high frequency region all the numerical models were found to be in good agreement with Goody and Efimtsov 1 models.

Belligoli *et. al.* [32] investigated the capabilities of DNS solver of OpenFOAM (Open source Field Operation And Manipulation) software package with two 2D and 3D generic test cases, i) Decay of Isotropic Turbulence (DIT) and ii) the Taylor-Green

(TG) vortex. They suggested simulations on 128^3 or even 256^3 cells for forced isotropic turbulence case. The Taylor-Green vortex case at low Reynolds number is reported as providing satisfying results.

2.4. REVIEW OF EXPERIMENTAL WORKS

The total root-mean-square pressure fluctuations p' is a parameter which is subject to greater experimental errors than individual frequency-spectral magnitude, being an integral of $\Phi(\omega)$, is subject to an accumulation of errors over the overall frequency range. In particular, it limits transducer resolution at higher frequencies. From the similarity relations for the frequency spectrum it is understood that appropriate pressure scale which make the dominant contribution to the overall r.m.s pressure, is the mean wall-shear stress (τ_w). Hence, p'/τ_w is used as most appropriate parameter in many early investigations which subsequently used as reference for the experimental results, as some significant uncertainties till remained in the early stage of experimentations.

As a preliminary discussion, it is pertinent to summarize the results of the experimental comparison of two types of pressure sensors, built by Bull & Thomas [33] used to measure wall-pressure fluctuations: so-called pinhole microphones, and flush-mounted transducers which introduce no discontinuity in the boundary surface.

Wall-pressure spectra were measured by various gadgets. Sometimes a pinhole in the boundary surface was used or a piezoelectric transducer having a sensing element of the same diameter as the pinhole was also used. All the configurations were individually calibrated. Thus measurements were made with i) a condenser microphone mounted in a cavity behind the surface pinhole, ii) a piezo-electric transducer mounted in a cavity behind the pinhole, iii) a piezo-electric transducer mounted behind the pinhole, but with no cavity, iv) a piezo-electric transducer mounted behind the pinhole (with no cavity), but with the pinhole filled with silicone grease to restore a continuous boundary surface, and v) the piezo-electric transducer mounted flush with the boundary surface with no surface discontinuity. The measured values of $\Phi(\omega)$ for the two configurations for which there was no surface discontinuity, cases iv and v, were indistinguishable from each other. Likewise, the measured values of $\Phi(\omega)$ for all open pinhole configurations, cases i, ii and iii, were indistinguishable from each other, but they were consistently higher than those obtained from transducers which introduced no surface discontinuity. It is concluded that the pinhole is responsible for local flow disturbances, scaling on inner layer variables, which leads to errors in the measured spectral densities of the wall-pressure field.

Farabee and Casarella [12] measured pressure with pinhole microphones, and the upper boundary of the universal frequency region based on them is 0.3, a value considerably higher than the Bull and Thomas value for the onset of pinhole errors in measured value of $\Phi(\omega)$. They questioned about the role of pinhole in causing error, and put their results, along with two other results obtained without the use of a pinhole by Emmerling, Meier and Dinkelacker and Schewe [34].

Farabee and Casarella [12] also observed that the values of p'/τ_w for pipe flow appear to be rather lower than those for boundary-layer flow. The results of Bull and Langeheineken [35] found to be in line with this observation.

Hu *et. al.* [36] performed an experiment in the Acoustic Wind-Tunnel Braunschweig (AWB) which was an open-jet low noise facility with a nozzle exit of 0.8 m x 1.2 m. The maximum flow velocity was 65 m/s. A 170 cm x 130 cm x 4 cm wood plate was aligned to the bottom side of the nozzle to allow boundary layer development. The boundary layer flow field was measured by a single hotwire probe at 154 cm behind the nozzle exit at mid span of the reference plate. Data were acquired at a sampling rate of 40 kHz for 13 s. Five different test velocities were set between 20.8 m/s and 62.4 m/s. Finally, $\Phi(\omega)$ for different cases were presented over the frequency range of 0-10000 Hz. Also, the non-dimensional pressure spectra, normalized with inner variables were presented by them.

Willmarth [37] conducted an experiment to measure wall-pressure fluctuations beneath a turbulent boundary layer on the outer surface of a cylinder aligned with a low-speed flow. The objective of the experiment is to determine the effect of transverse curvature on the wall-pressure fluctuations and on the structure of turbulence by comparison with measurements beneath flat plate boundary layers.

Bhat [38] investigated the turbulent boundary layer pressures on an aircraft surface using a seven microphone array. The results were broadly in agreement with laboratory measurements of flat plate wall pressure spectra.

Till 1972 all works were done considering small rectangular plate or small panel but for the first time Wilby and Gloyna [39] considered an airplane fuselage structure exposed to turbulent boundary layer to measure its vibration. The flight test results were presented in terms of power spectral density functions and broadband correlations.

Sulc, Hofrand and Benda [40] conducted experiment on a light aircraft and foun that much more intense pressure fluctuations are visible compared to those associated with the flat plate boundary layer behind local flow separations. However, this effect is unlikely to be as important on high speed aircraft, where the fuselage is much smoother.

An experimental investigation of sound generation from a flat, thin and smooth aluminium plate, excited on one side by a low Mach number turbulent flow was conducted by Cousin [41] in 1998. He performed the measurement in two main steps. Firstly, the flow in the test rig and wall pressure fluctuation was measured. In the second part of the test they determined the sound power emitted from the plate. They determined the power spectrum of the wall pressure fluctuations by using 1/8″ diameter microphones.

Lee and Sung [42] in 2001 conducted a laboratory measurement on wall pressure fluctuations in separation and reattachment of flows over a backward-facing

step. Arrays of 32 microphones along the stream as well as across the stream were utilized. The statistical properties of pressure fluctuation were scrutinized.

In 2011, Miller [43] conducted an experiment to determine the best empirical model to represents an aircraft environment. All the empirical models were compared with data from the Spirit Aerosystems, Inc. (Sprite) 6 x 6 in. duct at a range of Mach number. He concluded that Krichnan and Lueptow models are at the higher side whereas Bull and Willmarth and Wooldridge are at the lower side. He also concluded that Goody's model is best for aircraft industry.

Review till now include past works conducted analytically, empirical, semi-empirical and experimentally. Another family of researches adhered to finite element modeling of the problem. In the finite element modeling methods sometimes in-house finite element codes were developed by using various coding software for TBL modeling and structural response. In the next section finite element modeling related literatures are reviewed.

2.5. FINITE ELEMENT BASED NUMERICAL MODELLING

Weilin *et. al.* [44] resorted to finite element analysis of TBL problems. An elastic cylindrical shell and fluid loading was described by wavenumber frequency transfer function. A general expression of the TBL induced cross spectrum of the interior noise was derived. They found that the reduction in noise level is based on shell radius, shell thickness, absorption of material and the flow speeds.

TBL induced excitation in a clamped plate were predicted by Hambric *et. al.* [45] using random vibration analysis using a finite element model. The predicted vibrations were compared with the measured results made at the Ray Herrick Labs at Purdue University using a laser-Doppler vibrometer. The plate was flush-mounted into a wind tunnel wall and air was driven past the plate at a Mach number of 0.1. The measured boundary layer displacement thickness and flow velocity were used to estimate the wall pressure fluctuation auto-spectrum using the model developed by Smolyakov and Tkachenko [58]. They used two models for estimating the wall pressure cross-spectra: (i) Corcos model (ii) modified Corcos model. They observed that the modified Corcos model shows excellent agreement between the predicted and the measured vibration on the plate.

In 2002 Hardy *et. al.* [46] provided a complete description of the turbulent boundary layer (TBL) induced vibration by means of local energy method, for a simply supported thin plate. Ultimately, a numerical parametric survey was given by the for various internal loss levels and the link between results provided by them and SEA predictions of TBL structural induced vibration was discussed.

A numerical implementation for the vibration of a plate, excited by a turbulent boundary layer flow, was presented by Finnveden [47]. The results compare favorably with results from conventional modal analysis.

Hambric, Hwang and Bonness [48] published an article on TBL excitation. In this article special attention was given to the boundary condition and fluid velocity.

The vibration response of a TBL excited baffled flat rectangular plate was analyzed with two sets of boundary conditions: (a) all four edges clamped, and (b) three edges clamped and one edge free, with the flow direction perpendicular to the free edge. A finite element model with discretization sufficient to resolve the convective wavenumbers in the flow excitation field was used for the study. Three TBL wall pressure excitation models were applied to the plates to represent the cross-spectra of the wall pressures: (i) a modified Corcos model, which includes all wavenumber components of excitation; (ii) a low-wavenumber excitation model previously derived by one of the authors, which only models the wavenumber-white region of the modified Corcos model; and (iii) an equivalent edge force model which only models the convective component in the modified Corcos model. The TBL wall pressure auto-spectrum was approximated by using the model of Smolyakov and Tkachenko [58].

Yang Xin-ting [49] analyzed the flow noise in the interior fluid of a vector hydrophone towed linear array. They used Corcos's model which described the cross-spectrum of the TBL pressure fluctuations. Power spectrum of flow noise was calculated for point hydrophone, finite hydrophone and hydrophone array. It was observed that the numerical result shows that performance of the vector hydrophone towed linear array was very sensitive to the axial component of flow noise.

Rocha *et. al.* [50] discussed about the development of analytical models for prediction of cabin noise induced by TBL. Up to the year 2011, all the works were on the contribution of individual panel to the sound pressure level (SPL) but they introduced the contribution of multiple panels in SPL. Analytical prediction was presented for the interior SPL at different locations inside the cabin of a Blended Wing Body (BWB) aircraft, for the frequency range 0-1000 Hz. They observed that the average SPL, over the cabin volume increases with the number of vibrating panels.

Chen Meixia *et. al.* [51] presented a semi-analytical and semi-numerical method for calculating the vibration characteristic of structure excited by turbulent boundary layer based on random excitation theory. The power spectra density expression of the excitation caused by turbulent boundary layer given by Corcos was dispersed into matrix form as input. Combined with the frequency response function matrix considering fluid-structure interaction calculated by FEM/BEM methods, the power spectral density of the structure velocity was calculated. They found that the result from numerical method was quite identical with the analytical method. Thus, they used this method to calculate the vibro-acoustic characteristic of single cylindrical shells excited by turbulent boundary layer. The result shows that this semi-analytical and semi-numerical method was quite suitable for solving practical engineering projects the structure of which had a simple and regular outer shape but has quite complicated inner structures such as machinery, pipe system and so on.

Klabes *et. al.* [52] reviewed available published TBL models to understand the behavior of turbulent boundary layer. Furthermore, the influence of these different

models, numerically coupled to structures, was systematically examined. Firstly, systematical testing was performed on simply supported flat plates by using two methods; a method developed by Graham and a commercial software package using Statistical Energy Analysis (SEA). Secondly, tests on Airbus aircraft structures were performed by using SEA. Necessary aerodynamic input data were not taken from flat plate estimates but from CFD calculations as performed with DLR's in-house RANS solver TAU. Finally, calculation results of the structural vibration are compared with measured structural vibrations of the aircraft primary structure at cruise flight conditions. Apart from the results obtained from semi-empirical wavenumber-frequency models, the predictions with DLR's Fast Random Particle-Mesh Method (FRPM) of the spatio-temporal TBL behavior were also presented for Airbus aircraft in cruise flight conditions.

The methods of Principal Component Analysis (PCA) and Vibro-Acoustic Transfer Vectors (VATV) based on LMS Virtual Lab software were used to calculate the sound characteristics of a plate structure excited by TBL by Ll Zuhui *et. al.* [53]. The Corcos model of the wave number-frequency spectrum of the wall pressure field beneath the TBL was used to describe random excitation. By comparing the calculating time and sound pressure auto power spectra curves of the two methods, the following conclusions were obtained: both the VATV method and PCA method could be used effectively for the calculation of the flow-induced noise of structures excited by the TBL, and the results of the two methods match; the VATV method could quickly forecast the structure of flow-induced noise and takes up fewer computing resources than the PCA method; the PCA method could also obtain the structure vibration response in comparison with the VATV method. Their work could serve as a reference for the rapid prediction of the flow-induced noise of underwater structures.

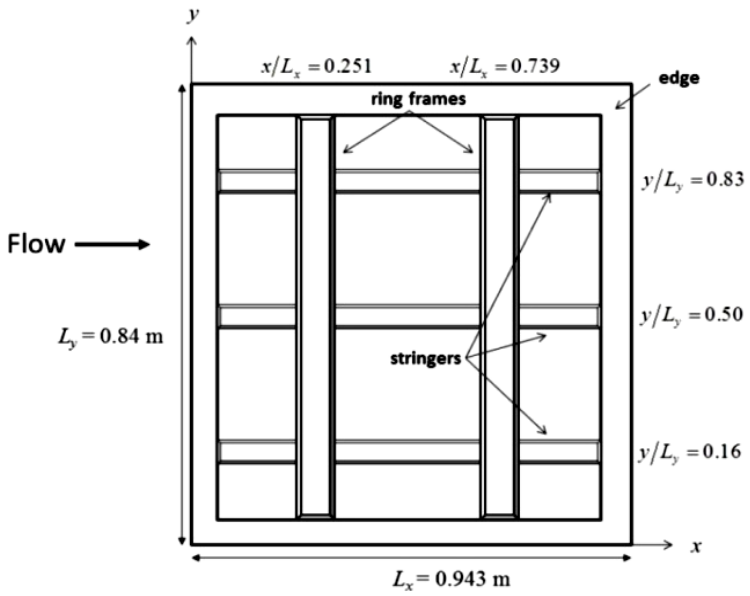

Fig. 2.1: Ribbed plate used by Hambric *et. al.* [54]

The models described in the earlier section are restricted to flat panels without stiffeners attachment. However, in modern day aerospace industry, ribbed plates or stiffeners are introduced to reduce the noise and vibration in aircraft. It is from this perspective a discussion is presented in this section to understand the behavior of TBL induced in aircraft cabin.

Rocha *et. al.* [50] investigated the effect of multi panel on TBL induced noise and vibration. The study concluded that the position of the panel as well as structural-acoustic coupling effects are important factors and the use of added mass in the structure can be a passive method of noise control.

In 2014, Hambric and Shepherd [54] introduced a ribbed plate which reduced the noise approximately by 10 dB. The ribbed plate is shown in the Fig.. 2.1 which had two ring frames and three stringers.

In the same year Bilong Liu *et. al.* [55] investigated the effect of ring frames, stringers, damping and curvature on the noise of aircraft panels under the excitation of the acoustic diffuse field and TBL respectively. They found that ring frames had almost no influence on sound transmission when subjected to excitation of an acoustical diffuse field while the ring frame had significant influences on TBL induced noise radiation. This conclusion based on numerical prediction.

It is evident from the discussion that the experimental result is bounded on the high end by the Kraichnan and Lueptow model and on the low end by the Bull and Willmarth and Wooldridge models. It is difficult to draw any conclusion which means that square pressure model suits best. The models of Efimtsov 1, Goody and Smol'yakov seemed to produce more reasonable values while Efimtsov 2 over-predicts the results. It was seen that Goody model is the most appropriate single-point wall-pressure spectrum model for aircraft. It can also be concluded after comparing the models of Corcos, Chase 1 and Smol'yakov that Chase 1 model also appears to be better for aircraft applications.

It is seen from the studies by Hambric *et. al.*[54], Liu *et. al.* [55] that the stiffener or ribbed panel reduces the noise level and vibration of the aircraft cabin. Multi panel structure or additional mass also reduces the noise pressure level as well as the vibration.

From the literature review it is observed that a number of researches worked on the TBL models while the other section of researches focused on structural response and sound pressure level due to TBL. One of the few works that deals both in the TBL model and structural excitation due to TBL induced pressure fluctuation can be attributed to Rocha *et. al.*[50]. The effect of change in Mach number and boundary condition on flow spectrum and structural response together are not clearly discussed in any of the presented literatures. So the objective of the present work is decided on the basis of the gaps seen in literature available.

2.6. OBJECTIVE

From the above discussion it is clear that the turbulence boundary layer induced structural vibration is very important for aircraft, submarine and automobile structures and it is seen that there are still a few gaps. So, in this present work TBL models and TBL induced structural vibration over a flat plate is studied for different flow parameter and structural parameters. Due to the limitation in computational facility, a flat plate is considered with number of elements delimited by available computing facility. Only three single-point wall pressure spectrum models are used, which are

(i) Smolyakov and Tkachenko's model
(ii) Efimtsov's first model
(iii) Goody's model

Three support conditions of a flat plate are considered in this present work, which are

(i) One edge clamped-three edges free
(ii) Four edges clamped (CCCC)
(iii) Four edges simply supported.

In this work the response of the structure determined for Mach number, M = 0.1, 0.3 and 0.5.Based on the obtained results of different parametric study the effect of various parameter is discussed.

Chapter – 3

Theory and Mathematical Modeling

3.1. THEORY AND MODELING

Prandtl's (1904) greatest achievement was to show the practical importance of viscous part of the flow had on the flow solution, which, up to that point of time, had been neglected to simplify the Navier-Stokes equations. Prandtl deduced that a reduced form of the governing equations could only be employed under certain conditions. From this, he derived the boundary layer equations, which hold under the following two conditions:

a. The viscous layer must be thin relative to the characteristic along-stream dimension of the object immersed in the flow, $\delta/L \leq 1$, where L is the characteristic length of the wall and δ is the distance away from the wall at which velocity attains its free-stream value.
b. The largest viscous term must be of the same approximate magnitude as any inertia term.

The velocity of fluid particles on the flat plate surface is zero and they act as a retardant to reduce velocity of adjacent particles in the vertical direction. These actions are followed by other particles until at the edge of the boundary layer where the particles velocity is 99% of the free stream velocity. Boundary layer can also be measured by more significant parameters. The main boundary layer parameters are as follows: The displacement thickness, δ^* is defined as the distance by which the external streamlines are shifted due to the presence of the boundary layer:

$$\delta^* = \int \left(1 - \frac{u}{u_\infty}\right) dy \tag{3.1}$$

The momentum thickness represents the height of the free-stream flow which would be needed to make up the deficiency in momentum flux within the boundary layer due to the shear force at the surface. The momentum thickness for an incompressible boundary layer is given by:

$$\Theta = \int \frac{u}{u_\infty}\left(1 - \frac{u}{u_\infty}\right) dy \tag{3.2}$$

The pressure fluctuations on the surface of the airplane, submarine or automobile due to TBL are confined to the boundary layer only. At the very first stage the flow is laminar but quickly changes to turbulent. A TBL can be divided into several regions with specific turbulence behaviors. A very thin layer near the wall is named laminar sublayer where the flow velocity decreases towards the surface. In this region turbulent fluctuation are damped. The outer region of the boundary layer, which contains turbulent flow, is referred to as fully turbulent zone, which is separated from laminar sublayer by buffer zone

The near wall behavior of the fluid is influenced by some physical parameters which are density (ρ), kinematic viscosity (ν), distance of the fluid particle from wall (y), and shear stress at the wall (τ_ω). The division of a turbulent boundary layer into regions is commonly identified by the definition of a non-dimensional velocity u^+ and a normal spatial surface coordinate y^+. These quantities are defined by

Inner layer – The law of the wall states that the average velocity of a turbulent flow at a certain point is proportional to the logarithm of the distance from that point to the wall.

Overlap layer – The logarithmic law of wall is valid for overlap region with approximately constant shear stress and far from the wall so as viscous effects to be negligible.

$$u^+ = \frac{1}{\kappa}\ln y^+ + C^+ \tag{3.3}$$

Where, C^+ is a constant and k is the von Karman constant.

$$u^+ = \frac{u}{U_\tau};\ y^+ = y\frac{U_\tau}{\nu} \tag{3.4}$$

Where the friction velocity is given by

$$U_\tau = \sqrt{\frac{\tau_\omega}{\rho}} \tag{3.5}$$

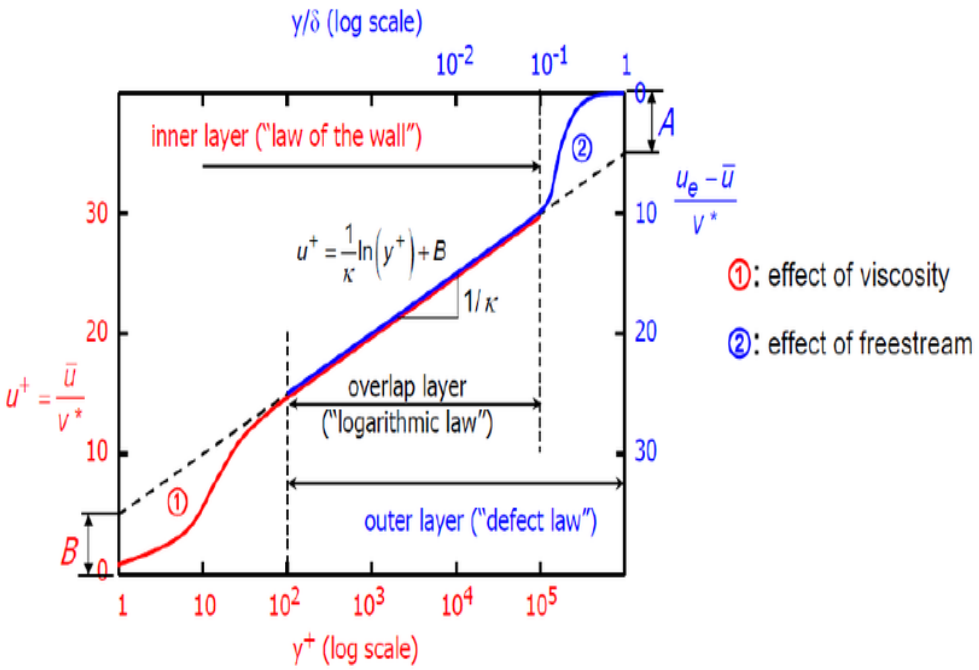

Fig. 3.1: A schematic representation of the turbulent boundary layer over flat plate

The values of some physical parameter such as boundary layer thickness (δ), the mean velocity ($\bar{u}$) etc. are needed in order to solve the pressure fluctuation under a TBL. In 1991 White [63] approximated the boundary layer thickness as

$$\delta = \frac{0.16\,x}{(R_{ex})\text{^}(1/7)} \tag{3.6}$$

and the velocity equation is given by

$$\bar{u} = U_{\infty}\left(\frac{y}{\delta}\right)^{\frac{1}{7}} \tag{3.7}$$

3.2. SIMULATION OF WALL-PRESSURE FLUCTUATIONS WITH EMPIRICAL/SEMI-EMPIRICAL MODELS

The three TBL models generally used as reported in the literature are *mean-square pressure models*, *single-point wall- pressure spectrum* and the *normalized wavenumber-frequency spectrum*. The Mean-square pressure is a measure of the total energy due to TBL pressure fluctuation where single-point wall pressure spectrum sorts the energy into frequencies and normalized wavenumber-frequency spectrum sorts the energy into wavenumbers. In this current work, several single point models are used. Only single-point wall-pressure models are used in this present work which is discussed below.

3.2.1. SINGLE-POINT WALL-PRESSURE SPECTRUM MODELS

The single-point wall-pressure spectrum models correspond to the distribution of the mean square pressure fluctuations with frequency. In this section few empirical models are presented. A theoretical spectral density model is required to compare the results of different models and numerical solutions.

The main objective of the section is to calculate the flow spectrum at a single-point at different times. The autocorrelation function for p(t), which is expected value of the pressure at time t and again t + τ can be explained as

$$R_{pp}(\tau) = E[p(t)\, p(t+\tau)] \tag{3.8}$$

The Fourier transform of $R_{xx}(\tau)$ and its inverse are given by

$$S_{pp}(\omega) = \frac{1}{\sqrt{2\pi}} \int_{-\infty}^{\infty} e^{-i\omega\tau} R_{pp}(\tau) d\tau \tag{3.9}$$

and

$$R_{pp}(\tau) = \frac{1}{\sqrt{2\pi}} \int_{-\infty}^{\infty} e^{i\omega\tau} S_{pp}(\omega) d\omega \tag{3.10}$$

where $S_{pp}(\omega)$ is called the spectral density of the pressure process, which is a function of angular frequency. The fundamental definition of the auto-correlation function provides

$$E\,[p^2] = \int_{-\infty}^{+\infty} S_{pp}(\omega)\, d\omega \tag{3.11}$$

This can be written as,

$$E\,[p^2] = \int_{0}^{\infty} W_{pp}(f)\, df \tag{3.12}$$

Where f is the frequency (Hz), and $W_{pp}(f)$ is the equivalent one-sided spectral density function. Now, if the single-point power spectrum is defined by $\phi_{pp}(\omega)$, then one can obtain

$$\phi_{pp}(\omega) = 2\, S_{pp}(\omega) \tag{3.13}$$

and the power spectrum level can be calculated by

$$W_{pp}(f) = 2\,\pi\,\phi_{pp}(\omega) \tag{3.14}$$

Among the all single-point power-spectrum models describe in the literature review only three models are considered in the present work. The three models which used to obtain the flow spectrums are as follows:

A. Smolyakov and Tkachenko's model
B. Efimtsov's model
C. Goody's model

These three models are described below.

A. Smolyakov and Tkachenko Model

In the 1992, Smolyakov and Tkachenko introduced a Φ (ω) which is given below

$$\Phi\,(\omega) \approx \left(\frac{\tau_\omega^2 \delta^*}{U_0}\right)\left(\frac{5.1}{1+0.44\,(\frac{\omega\delta^*}{U_0})^{7/3}}\right) \tag{3.15}$$

Where U_0 is the free-stream velocity, δ^* is the boundary layer displacement thickness, τ_ω is the wall shear stress which can be estimated from TBL flow with zero pressure gradient using the empirical relations $R_{e\delta} \approx 8U_0\delta^*/\vartheta$ and $\tau_\omega \approx 0.0225\rho U_0^2/R_{e\delta}{}^{0.25}$, where $R_{e\delta}$ is the boundary layer thickness Reynolds number, ν is the kinematic viscosity, and ρ is the fluid density.

B. Two models of Efimtsov

Efimtsov [15, 16] gives two single-point wall-pressure spectrum models on which the first model is referred as first model of Efimtsov or Efimtsov 1 [15] and the second one is referred as second model of Efimtsov or Efimtsov 2. Efimtsov stated that a single-point wall-pressure spectrum model should be dependent on Mach number (M), Reynolds number (Re), and Strouhal number (S_h). The Strouhal number is S_h = ωδ /Uτ. Efimtsov collected a series of flight test data in the range of Mach numbers of M = 0.41 to 2.1 with Reynolds number of $Re_x = 0.5 \times 10^8$ to 4.85×10^8. The pressure fluctuations were measured at various zones along the fuselage. Efimtsov' proposed the following equation:

$$\Phi\,(\omega) = \frac{0.01\tau_\omega^2\delta}{U_\tau[1.0+0.02(\omega\delta/U_\tau)^{2/3}]} \tag{3.16}$$

$$\text{Where,} U_\tau(x) = \text{Friction velocity} = U_\infty\sqrt{\frac{C_f(x)}{2}},$$

$$\tau_\omega(x) = \text{Mean wall shear stress} = \frac{1}{2}\rho U_\infty^2 C_f(x),$$

$$C_f(x) = \text{Friction coefficient} = 0.37(Log_{10}R_{ex})^{-2.584}$$

and δ(x)=TBL thickness = 0.37 x $R_{ex}^{-\frac{1}{5}}[1 + (\frac{R_{ex}}{6.9\ x\ 10^7})^2]^{\frac{1}{10}}$

Efimtsov 2 [16] was an updated model in which the principal independent variables are the Strouhal number and the Reynolds number:

$$\Phi(\omega) = \frac{2\pi\alpha U_\tau^3 \rho^2 \delta\beta}{[1+8\alpha^3(\frac{\omega\delta}{U_\tau})]^{1/3}+\alpha\beta R_{e_\tau}[(\frac{\omega\delta}{U_\tau})/R_{e_\tau}]^{10/3}} \quad (3.17)$$

Where, $Re_\tau = \frac{\delta U_\tau}{\nu_w}$; $Re_{\tau 0} = 3000$;

$$\beta = [1+(\frac{Re\tau 0}{Re\tau})]^{1/3}; \alpha = 0.01;$$

$$\nu_w = \nu\frac{\rho}{\rho_w}(\frac{T_w}{T_\infty})^{\Upsilon}; \Upsilon = 0.905;$$

$$T_w = T_\infty(1 + r\frac{k-1}{2}M^2); r = 0.89;$$

$$k = 1.4; \rho_\omega = \rho\frac{T_\infty}{T_\omega}$$

C. Goody Model

In this present work Goody's model (2004) is also used which is a modified form of the Chase-Howe model. Goody [16] proposed an empirical model of the single-point wall-pressure spectrum beneath a two-dimensional, zero-pressure-gradient boundary layer which was based on the experimental surface pressure spectra measured by seven research groups. To get better agreement with the experimental data Goody modified the Chase-Howe model with the following considerations in mind:

1) A term was added to the denominator so that spectral levels decay as ω^{-5}as $\omega\rightarrow\infty$.
2) The exponents in the denominator were changed to better agreement with the measurement p spectral behaviour at middle frequencies (the overlap range).
3) A multiplication constant was also added to the model function to raise the spectral levels at all frequencies so that they better agree with the experimental data.
4) The Reynolds number trends that exist in the data are accurately reflected.

The functional from, which incorporates the preceding considerations, is given below

$$\frac{\varphi(\omega)U_e}{\tau_\omega^2\delta} = \frac{C_2(\omega\delta/U_e)^2}{[C_1+(\omega\delta/U_e)^{0.75}]^{3.7}+[C_3(\omega\delta/U_e)]^7} \quad (3.18)$$

Where C_1, C_2, C_3 vary with Reynolds number. The above equation it is increases as ω^2at the lowest frequencies and decays as approximately $\omega^{-0.7}$ at middle frequencies and decays as ω^{-5} at the highest frequencies. The ratio of C_1 to C_3 determines the size of the overlap range. Goody used the model parameter C_1=0.5, C_2=3.0, C_3=1.1$R_T^{-0.57}$ and the final form of the empirical model is

$$\frac{\varphi(\omega)U_e}{\tau_\omega^2\delta} = \frac{3.0\ (\omega\delta/U_e)^2}{[0.5+(\omega\delta/U_e)^{0.75}]^{3.7}+[(1.1R_T^{-0.57})(\omega\delta/U_e)]^7} \quad (3.19)$$

Where R_T is define as ratio of timescales, as R_T increases, the low-frequency, outer-layer-scaled frequency range moves away from the high-frequency, inner-layer-scaled frequency range and the size of the overlap range increases. The approximate ratio of outer-layer-to-inner-layer timescale:

$$\left(\delta/U_e\right)/\left(\vartheta/u_\tau^2\right) = u_\tau^2\delta/U_e\vartheta = \left(\frac{u_\tau}{U_e}\right)\left(u_\tau\delta/\vartheta\right) = (u_\tau\delta/\vartheta)\sqrt{C_f/2} \equiv R_T \quad (3.20)$$

Where C_f = Skin friction coefficient, τ_ω/Q_e

δ = boundary-layer-thickness, u_τ = friction velocity, $(\tau_\omega/\rho)^{0.5}$

ϑ = kinematic viscosity, (μ/ρ);U_e = velocity at the boundary-layer edge

Goody use Blasius's empirical equation for the resistance coefficient in the pipe flow in the forms

$$C_f = 0.045\ (\nu/U_e\delta)^{1/4};\ \delta/\chi = 0.37\ (\nu / U_e x)^{\frac{1}{5}}; \quad (3.21)$$

$$R_T = 0.129\ (U_e\theta/\vartheta)^{\frac{3}{4}}\ ;R_T = 0.0107\ (U_e x/\vartheta)^{\frac{3}{4}} \quad (3.22)$$

3.3. TBL INDUCED STRUCTURAL VIBRATION

Pressure fluctuations beneath the TBL act as external loading on the structure and excite it. As the turbulence is random in nature, the resulting pressure signal in time domain is also random, and it contains energy for a wide range of frequency. Thus, it perturbs the structure in that large range of frequency, though the present work will be limited to the low-mid frequency range (0 – 500 Hz). In this work the TBL induced structural vibration is obtained by coupling the flow spectrum with the frequency response function. The flow spectrum is obtained by using the models discussed above. To obtain the frequency response function of the structure mode shape data is required. This mode shape data is obtained from the ANSYS Parametric Design Language (APDL). The mathematical model of frequency response function is discussed below.

3.3.1. FREE VIBRATION ANALYSIS

The objective of this section is to obtain frequency response function (FRF) or relation between displacement and exiting force. According to the model of modal analysis every structure consists of mass, springs and dampers which is shown in Fig.. 3.5. The matrix form of the structural equation subjected to dynamic loading can be written as:

$$[\mathrm{m}]\ddot{x} + [C]\dot{x} + [K]x = F \quad (3.23)$$

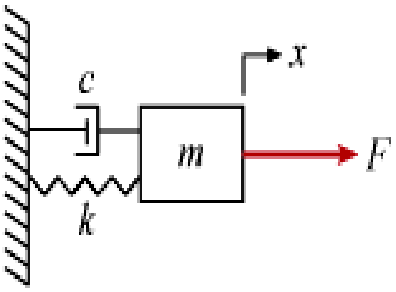

Fig. 3.2: Single degree of freedom system

Where [m], [C], [K] are represents the mass, damper and stiffness matrixes respectively. x, $\dot{x}$, $\ddot{x}$ are the displacement, velocity and acceleration vector respectively for n discretized points or degrees of freedom (DOF). F is a vector that represents the force applied on each DOF in the time domain. Dividing the equation (3.23) by m and rearranging the terms it can be written as:

$$\ddot{x} + 2\xi\,\omega_n\dot{x} + \omega_n^2\,x = {}^{F}/_{m} \tag{3.24}$$

Where, $\omega_n = \sqrt{{}^{k}/_{m}}$ is natural angular frequency and $\xi = {}^{C}/_{2\sqrt{Km}}$ is the damping ratio. Now, shift the above equation (3.24) to modal domain i.e.,,. by submitting the x = φ. q and F = $\overline{F_0}\,e^{i\omega t}$ equation (3.25) is obtained, where, q is the model displacement, φ is mode shape data, $\overline{F_0} = \varphi^T F_0$, $\overline{F_0}$ = initial modal force, φ^T= mode shape data and F_0 = intial force.

$$\ddot{q} + 2\xi\omega_n\dot{q} + \omega_n^2\ \mathrm{q} = \frac{\overline{F_0}}{m}\,e^{i\omega t} \tag{3.25}$$

By considering q = $q_0 e^{i\omega t}$, where q is the modal displacement and q_0 = initial modal displacement. Putting the q, $\dot{q}$, $\ddot{q}$ and by rearranging in the equation (3.25) the equation below can be written.

$$\frac{q_0}{\varphi^T F_0} = \frac{1}{\bar{m}(-\omega^2 + 2\xi\omega_n\omega + \omega_n^2)} \tag{3.26}$$

From the equation (3.26) it can be writing,

$$\frac{X}{F_0} = \frac{\varphi\,\varphi^T}{\bar{m}(-\omega^2 + 2\xi\omega_n\omega + \omega_n^2)} \tag{3.27}$$

From the above discussion it is clear that the frequency response function can be calculated by using following formation,

$$[\mathrm{X}]_{n\,\mathrm{x}\,1} = [\mathrm{H}]_{n\,\mathrm{x}\,\mathrm{n}}\,[\mathrm{F}]_{1\,\mathrm{x}\,n} \tag{3.28}$$

3.3.2. CROSS-SPECTRAL DENSITY USING COHERENCE FUNCTION

In this present work the process is considered as a temporally stationary and a coherence function ($\Gamma\,(\xi_1, \xi_2, \omega\,)$) is used to obtain cross-spectral density

($\Phi_{pp}(x_\mu, x_\nu, \omega)$) from averaged auto-spectral density ($\bar{\Phi}_{pp}(\omega)$) between the loaded pointsx_μ and x_ν as introduced by Hambric *et. al.* [49]:

$$\Phi_{pp}(x_\mu, x_\nu, \omega) = \bar{\Phi}_{pp}(\omega)\, \Gamma\,(\xi_1, \xi_2, \omega) \cong \sqrt{\Phi_{pp}(x_\mu, \omega)\Phi_{pp}(x_\nu, \omega)}\Gamma\,(\xi_1, \xi_2, \omega) \tag{3.29}$$

Where, the Averaged auto-spectral density $\bar{\Phi}_{pp}(\omega)$ is approximately the average of $\Phi_{pp}(x_\mu, \omega)\Phi_{pp}(x_\nu, \omega)$ and ξ_1, ξ_2 are the stream-wise and span-wise separation distance between pointsx_ϑ and x_μ.

$\Gamma\,(\xi_1, \xi_2, \omega)$ is the coherence function of the fluctuating wall pressures, such that

$$\Gamma\,(\xi_1, \xi_2, \omega) = \frac{1}{2\pi}\int_0^\infty R(\xi_1, \xi_2, \omega) e^{-i\omega\tau} d\tau \tag{3.30}$$

Where R indicates the space-time correlation of the fluctuation pressure field and Γ depends only on frequency and ξ_1, ξ_2 are the separation vector between points x_ϑ and x_μ in the plane of flow. As per several investigators$\Gamma\,(\xi_1, \xi_2, \omega)$ may be separable in stream and span wise directions. In 1963 Corcos proposed model which is given below:

$$\Gamma\,(\xi_1, \xi_2, \omega) = A\,(\omega\xi_1/U_c)\; B\,(\omega\xi_3/U_c) \tag{3.31}$$

Where U_c is the average convective velocity of the flow is a function of free stream velocity (U_0), angular frequency (ω) and boundary layer displacement thickness (δ*). Bull in 1967 used a approximated formation of convection velocity as a function of ω, δ*, U_0

$$U_c \cong U_0\,(0.59 + 0.30e^{-0.89\omega\delta^*/U_0}) \tag{3.32}$$

As per Corcos the function A and B is an exponentially decaying oscillating function in the direction of flow and in the cross-flow direction.

$$A(\omega\xi_1/U_c) = e^{-\alpha_1|\frac{\omega\xi_1}{U_c}|}e^{\frac{\omega\xi_1}{U_c}} \tag{3.33}$$

And

$$B(\omega\xi_3/U_c) = e^{-\alpha_3|\frac{\omega\xi_3}{U_c}|} \tag{3.34}$$

3.3.3. STRUCTURAL RESPONSE

While discussing the development of analytical models to predict submarine, automobile or aircraft cabin noise induced by the external turbulent boundary layer (TBL), structural response and acoustic pressure inside the cabin due to turbulent flow excitation is obtained by using the equations shown in below.

$$S_{ww}(\omega) = {H_W}^*(\omega) S_{tbl}(\omega) {H_W}^T(\omega) \tag{3.35}$$

$$S_{PP}(\omega) = {H_P}^*(\omega) S_{tbl}(\omega) {H_P}^T(\omega) \tag{3.36}$$

Where $S_{ww}(\omega)$ is the PSD matrix of the plate displacement, $S_{PP}(\omega)$ is the PSD matrix of the acoustic pressure, $S_{tbl}(\omega)$ is the PSD matrix of the TBL pressure, and superscripts * and T denote Hermitian conjugate and matrix transpose, respectively. $H_W(\omega)$ and $H_P(\omega)$ are frequency response matrices.

A baffled flat plate excited by TBL flow is considered as shown in Fig.. 3.3. Assuming wall-pressure fluctuations under TBL as stationary, the PSD of displacement response between any two degrees of freedom on the plate is shown in equation 3.37.

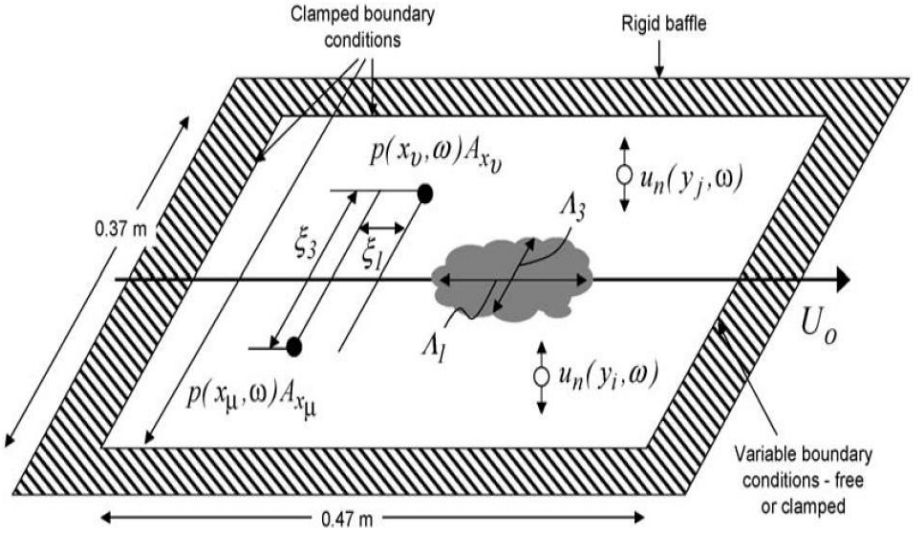

Fig. 3.3: TBL-excited baffled flat plate, pressures applied at points x_μ and x_ϑ, normal response at point y_i and y_j [48]

$$G_{uu}(y_i, y_j, \omega) = \iint H_{u,F}(y_i|x_\mu, \omega)\, \Phi_{pp}(x_\mu, x_\nu, \omega) H_{u,F}(y_j|x_\nu, \omega) dA_\mu dA_\nu \qquad (3.37)$$

Where, G_{uu} is the displacement response cross-power spectral density between DOF y_i and y_j, $H_{u,F}(y_j|x_\nu, \omega)$ and $H_{u,F}(y_j|x_\nu, \omega)$ are the frequency response functions relating displacement at response DOF y_i and y_j to forces applied at loaded points x_μ and x_ν (excitation point) , and $\Phi_{pp}(x_\mu, x_\nu, \omega)$ is the TBL pressure cross-power spectral density function applied to all loaded points. The response cross-power spectral density was approximate by double summation over all loaded area.

$$G_{uu}(y_i, y_j, \omega) \cong \sum_{\mu=1}^{N} \sum_{\nu=1}^{N} H_{u,F}(y_i|x_\mu, \omega) \Phi_{pp}(x_\mu, x_\nu, \omega) H_{u,F}(y_j|x_\nu, \omega)\, A_\mu A_\nu \qquad (3.38)$$

Where, A_μ and A_ν are the incremental surface areas of loaded point. In this present work the above formation is used to obtain displacement response cross-power spectral density. The final results can be obtained by using the above equation.

Chapter – 4

Results and Discussion

4.1. INTRODUCTION

The design of any structural component subjected to turbulent flow or laminar flow requires accurate predictions of fluid flow around its surface. The behaviour of air over the surface of the vehicle varies with parameters like temperature, velocity, density, etc. Like in case of airborne vehicles since the density of air varies with the altitude, hence the vehicle experiences vastly different flow regimes. Reproduction of these varied flow parameters in ground-based laboratories is both expensive and technically challenging. This is where computational models come into picture. Not only they provide fairly accurate results but are also extremely cheap as compared to their experimental counterparts. In the present work a flat plate, in a three-dimensional domain is studied for determination of structural vibration due to turbulent flows.

The different steps followed to obtain the structural response are as follows:

1) Obtaining the free vibration parameter of the structure using FE analysis carried out in ANSYS.
2) Calculation of frequency response functions of the structure from the obtained free vibration parameter using an in-house MATLAB code.
3) Development of PSD of TBL flow using in-house MATLAB code.
4) Development of a separate in-house MATLAB code to estimate the structural response which performing a coupled fluid-structure interaction model.

4.2. DETAILS OF THE STRUCTURE

The structural form considered in the present analysis has the following parameters:

4.2.1. DIMENSIONS OF THE PLATE

The length, width and the thickness of the plate is given below:

Table 1: Dimensions of the plate

Length, a (m)	Width, b (m)	Thickness, t (m)
0.47	0.37	0.00159

4.2.2. MATERIAL PROPERTIES

The material properties of the plate are discussed below:

- Material: Steel;
- Density (Kg/m^3): 7850;
- Modulus of Elasticity (GPa): 200
- Poisson's Ratio: 0.3

4.2.3. BOUNDARY CONDITION

Three different boundary conditions are considered in the present work. The schematic of each one of the boundary conditions are shown in the Fig. 4.1.

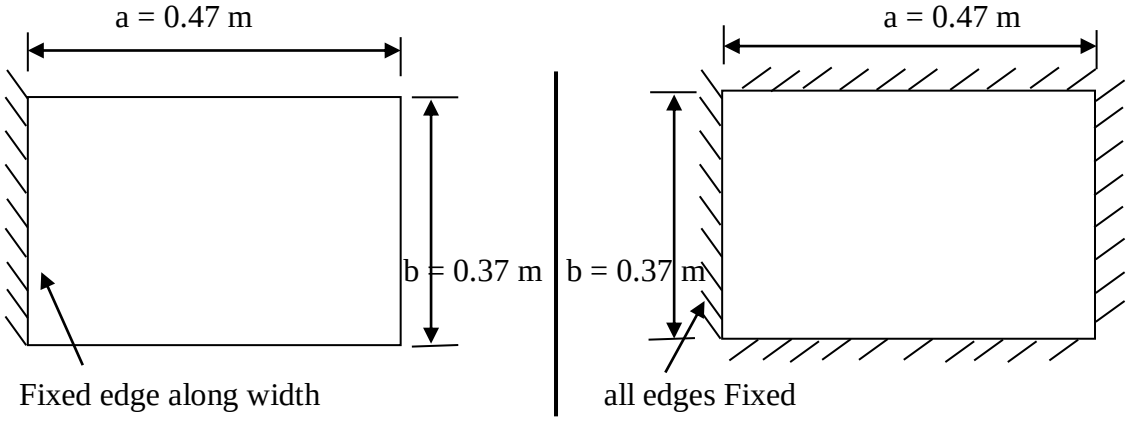

(i) Cantilever Boundary Condition (ii) CCCC Boundary Condition

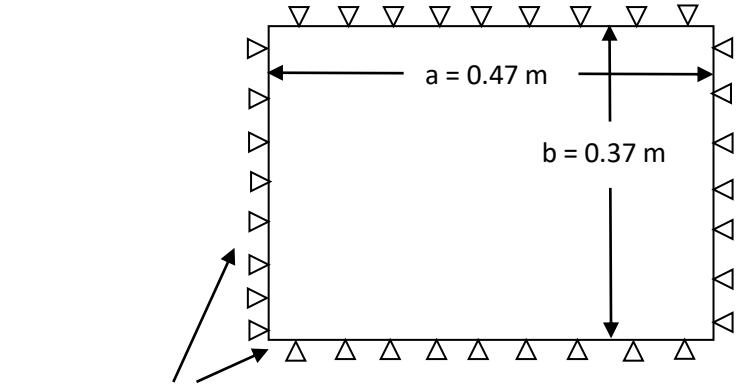

(iii) All edges simply supported

Fig. 4.1: The Steel plate with dimensions, three support conditions

4.3. NUMERICAL RESULTS

4.3.1. FREE VIBRATION ANALYSIS

Numerical analysis of the plate structure for free vibration analysis is performed using ANSYS Parametric Design Language (APDL) from where the frequency and mode shape data are obtained. Frequency response function (FRF) is estimated by using the frequency – mode shape data in MATLAB environment. A convergence study is performed by using different mesh division. The variation of natural frequency with the numbers of elements for CCCC boundary condition is shown in Table 2. Increase in numbers of elements, demands better computational facility and higher computational time. Due to the limitation in computational time and facility, for further study, the plate structure is discretized into 60x6 numbers of elements i.e., 61 numbers of nodes in stream-wise direction and 7 numbers of nodes in cross direction. So, the total number of node considered is 427. This frequency response function is coupled with the cross-power spectral density to get the response of the structure as

discussed in the previous chapter. Structural response is determined for low to mid frequency range 0-500Hz. As discussed earlier three support conditions are considered.

Table 2: Convergence study

PLATE DIMENSION - 0.47 x 0.37 x 0.00159, B.C. – CCCC, Max. freq - 500Hz						
Element / **Mode**	**94 x 74**	**60 x 40**	**60 x 20**	**60 x 14**	**60 x 10**	**60 x 6**
1	83.71	83.79	84.06907	84.45745	84.93949	88.1812
2	145.35	145.59	145.7194	145.9056	146.1379	147.7326
3	193.19	193.96	196.5706	200.3209	205.0978	241.2427
4	245.79	246.67	246.6823	246.7012	246.7268	246.9596
5	249.97	250.72	252.8443	255.9149	259.8417	290.1089
6	345.42	346.54	348.0925	350.3401	353.2268	375.9724
7	360.18	363.35	373.7731	384.6609	384.4911	383.4451
8	382.47	384.89	384.7992	389.2212	409.7199	499.8669
9	414.81	417.74	427.3056	441.5175	460.4447	*
10	478.44	480.84	481.796	483.1941	485.0051	*

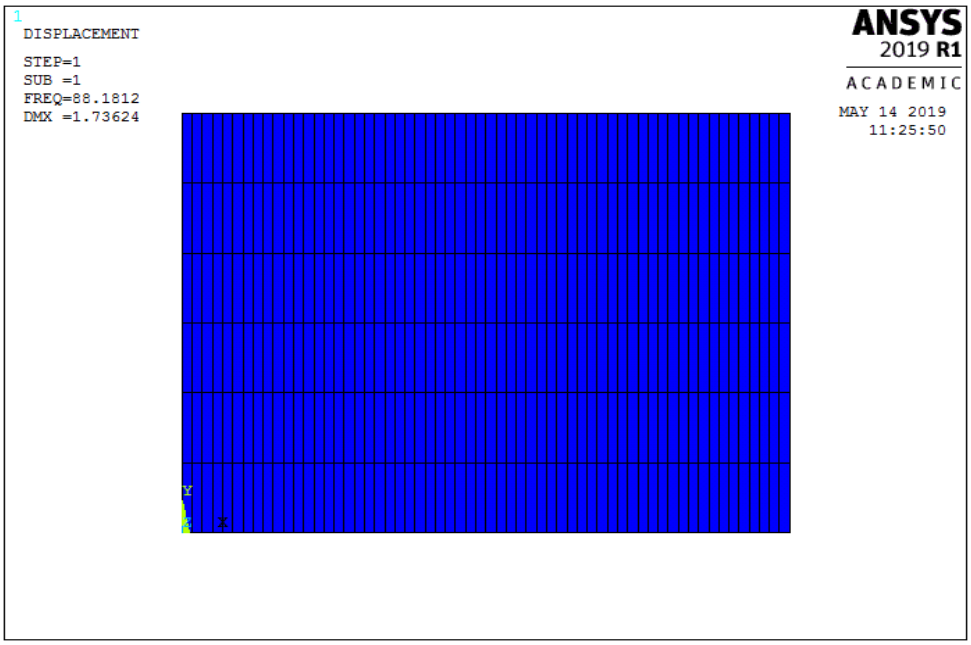

Fig. 4.2: Free vibration analysis of plate in APDL and meshing details

The natural frequency corresponding to the numerical models for different boundary conditions are given in the Table 3.

Table 3: Natural frequency of the plate for various support conditions

Support Condition / Modes	Cantilever Support	CCCC	All edges Simply Supported
1	9.8830	88.1812	46.0649
2	20.3553	147.7326	97.5865
3	51.4417	241.2427	145.4644
4	66.8852	246.9596	183.6868
5	82.5993	290.1089	195.3184
6	118.6493	375.9724	278.6409
7	128.3743	383.4452	304.6973
8	197.1115	499.8669	368.2781
9	209.2370	-	395.7593
10	222.4999	-	414.7331
11	228.1831	-	461.0883
12	274.7842	-	492.3650
13	298.8311	-	-
14	348.7300	-	-
15	361.1289	-	-
16	429.6770	-	-
17	454.1168	-	-

4.3.2. TBL MODELS

As discussed earlier three TBL models are developed in MATLAB environment. The coherence function introduced by Hambic *et. al.* [48] is applied to the all the three single-point wall pressure spectrum considered here to get the cross-power spectral density. The three TBL models i.e., Smolyakov and Tkachenko [58], Efimtsov [15] and Goody's models [21] are studied in this present work and are discussed below:

In 2007, Hambric *et. al.* [59] considered several empirical models of wall pressure autospectra under zero pressure gradient TBL flow. They plotted the model of Smolyakov and Tkachenko against several sets of measured data using mixed variable scaling which is shown in Fig. 4.3 below.

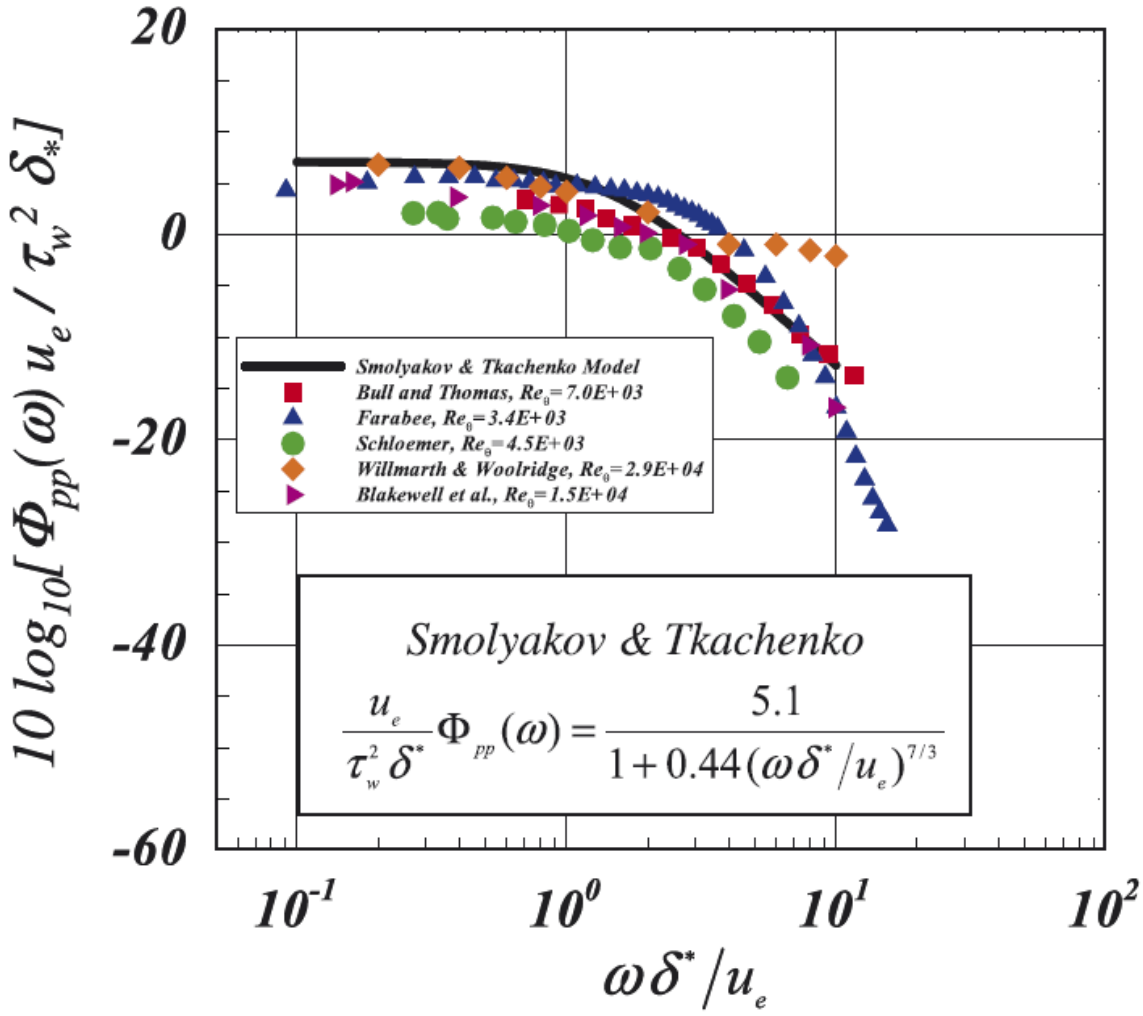

Fig. 4.3: Smolyakov and Tkachenko single point pressure spectrum model Vs measured data [59]

Using the code developed in MATLAB and putting wall shear stress $\tau_\omega = 0.0225\rho U^2/R_{ed}^{0.25}$; $R_{e\delta} = 8U\delta/\vartheta$as in the Smolyakov and Tkachenko's single-point wall-pressure spectrum model a similar graph is obtained as shown in Fig. 4.4. Hambric *et. al.*[59] considered the value of displacement thickness (δ*) and free

stream velocity as 2.7mm and 35.8 m/sec respectively, which are kept same in the present work.

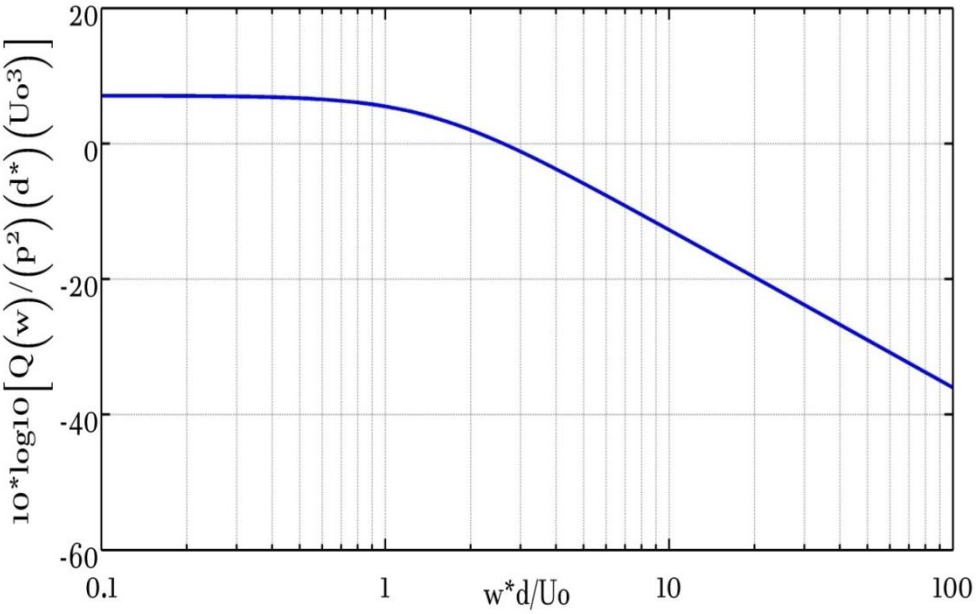

Fig. 4.4: Smolyakov and Tkachenko single point pressure spectrum model (Present work)

Similarly, Goody [21] also compared his model with the experimental data which is shown in the Fig. 4.5.

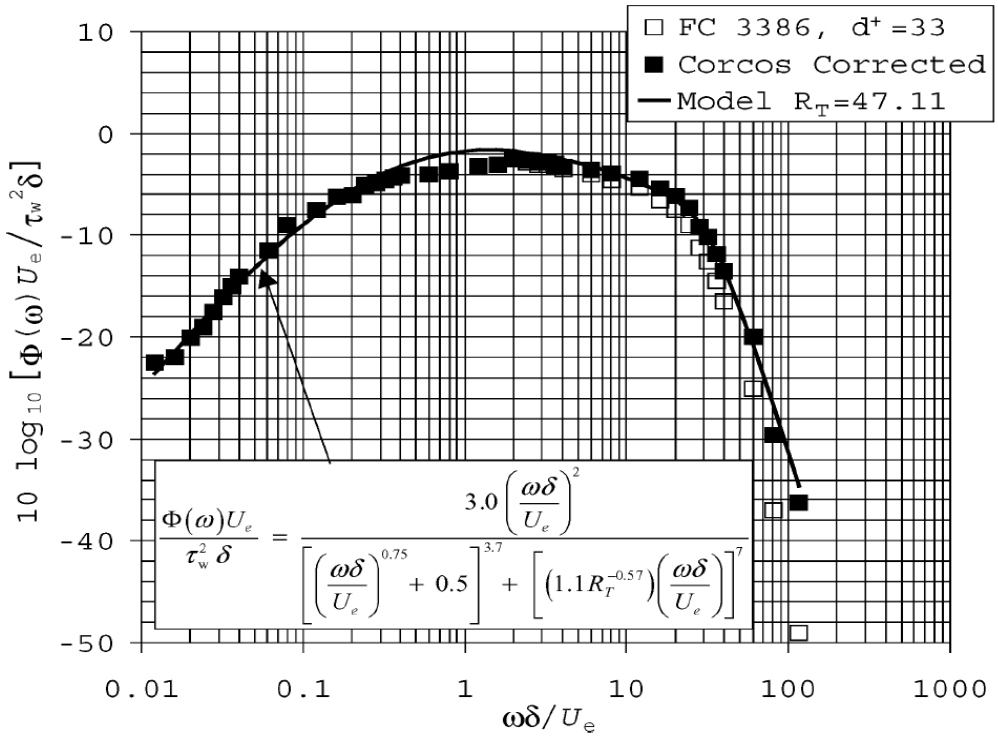

Fig. 4.5: Comparison of Goody's model with the data of Farabee and Casarella: $d^+ = 33$, $R_{e\Theta}=3.386 \times 10^3$, and $R_T = 47.11$. [21]

Goody's model [21] is discussed earlier in Chapter 3. Using the code developed in MATLAB and putting wall shear stress $\tau_\omega = 0.0225\rho U^2/R_{e\delta}^{0.25}$; $R_{e\delta} = 8U\delta/\vartheta$; $\delta = 0.37\text{x}(\nu/Ux)^{0.2}$ and $R_T = 47.11$ in the Goody's model [21] the single point power spectrum is obtained at mach number 0.5 as shown in Fig. 4.6. The obtained results show good relation with those shown in Fig. 4.5.

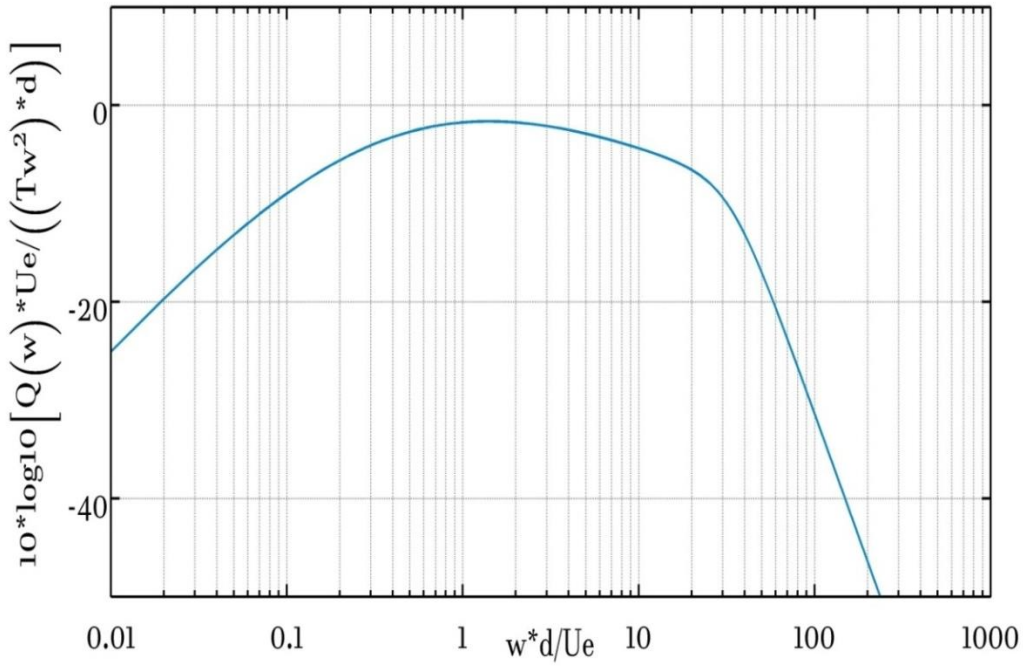

Fig. 4.6: Goody's model (Present work)

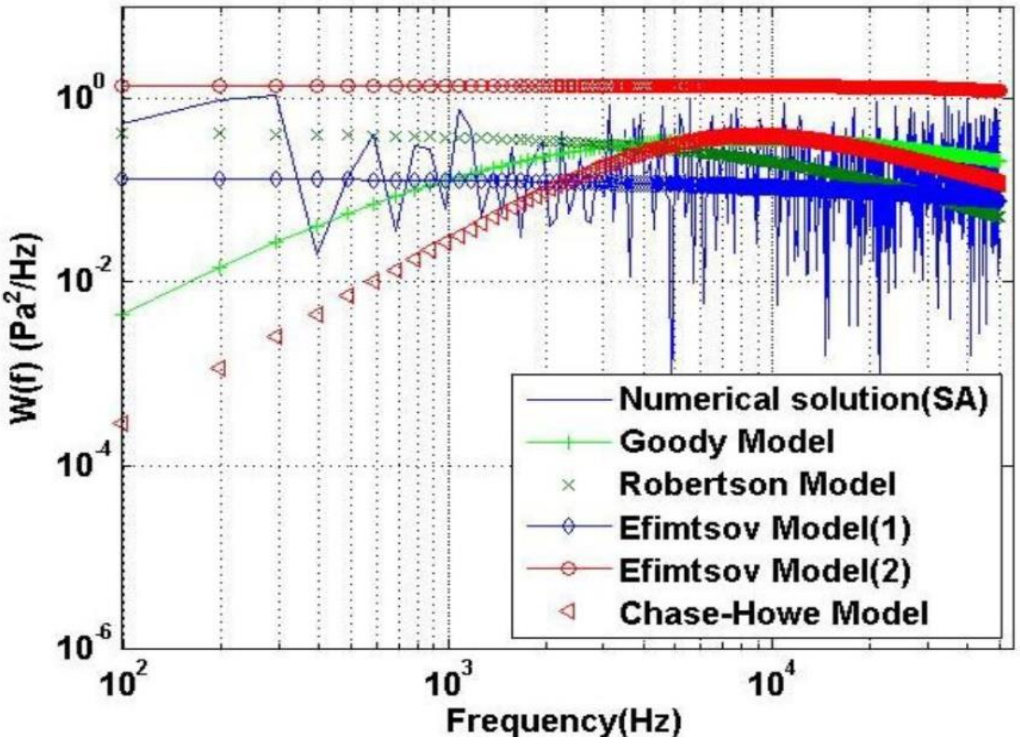

Fig. 4.7: Efimtsov 1 experimental pressure spectral density at U_0 = 170 m/sec [31]

Similarly Niloufar Mahmoudnejad [31] and Teresa S. Miller [43] in 2011 compared the Efimtsov first model (discussed in 3.2.1 (B)) with several single-point pressure spectrum models numerically and experimentally. Niloufar [31] considered a plate of dimension 0.3 x 0.05 meter with a domain height of 0.03m and measured single-point wall-pressure spectrum at a point 0.25m in stream-wise direction from the plate edge. The experimental power spectral density can be obtained by multiplying 2π to the single-point wall pressure spectrum and substituting $\omega = 2\pi f$.

In the present work the Efimtsov [15] single-point wall pressure spectrum is calculated by code developed in MATLAB. The result obtained from MATLAB shows a good agreement with the numerical data obtained by Niloufar [31], which is shown in Fig. 4.8.

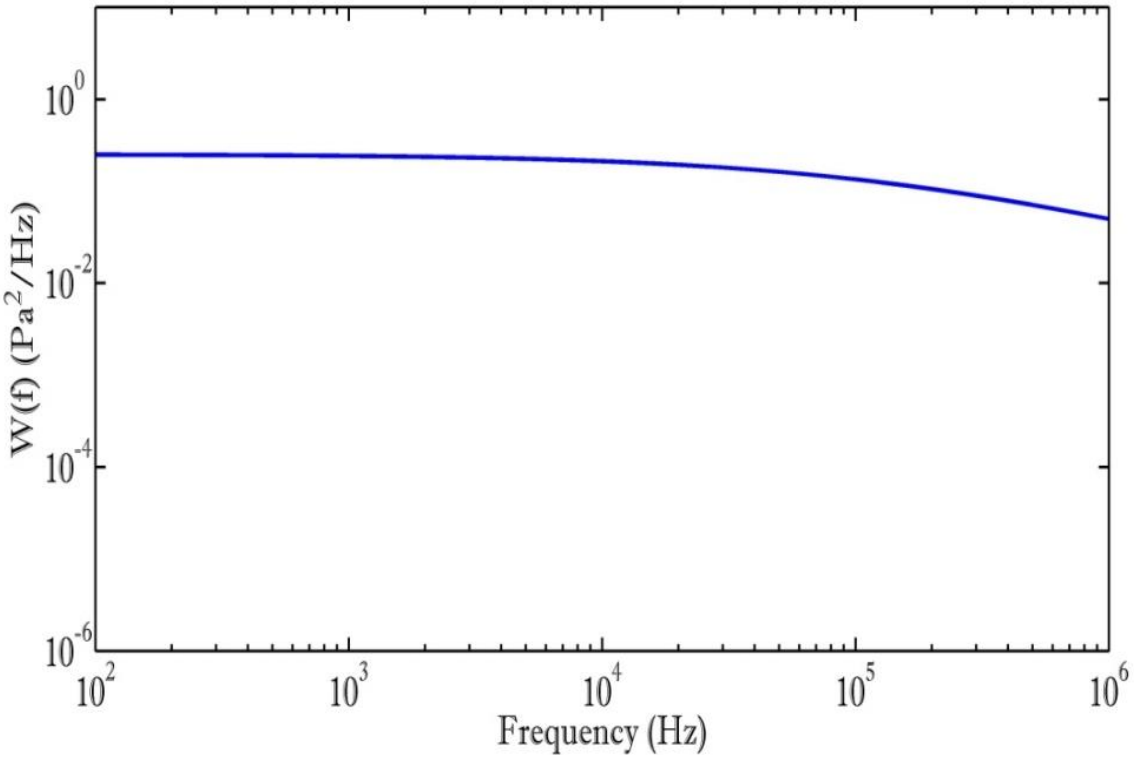

Fig. 4.8: Efimtsov first Model (Efimtsov-1) at free stream velocity (U_0) = 170 m/sec (Present work)

Subsequently results are obtained for different Mach number based on Efimtsov's first model [15] and the results compared with the results obtained by Miller [43], experimentally. From the comparison it is clearly seen that up to 2 x 10^3 Hz it shows good agreement, after that it degenerate. However, in this work the structural response of estimate for low to mid frequency range (0-500Hz). So the result of the present work can be used with accuracy.

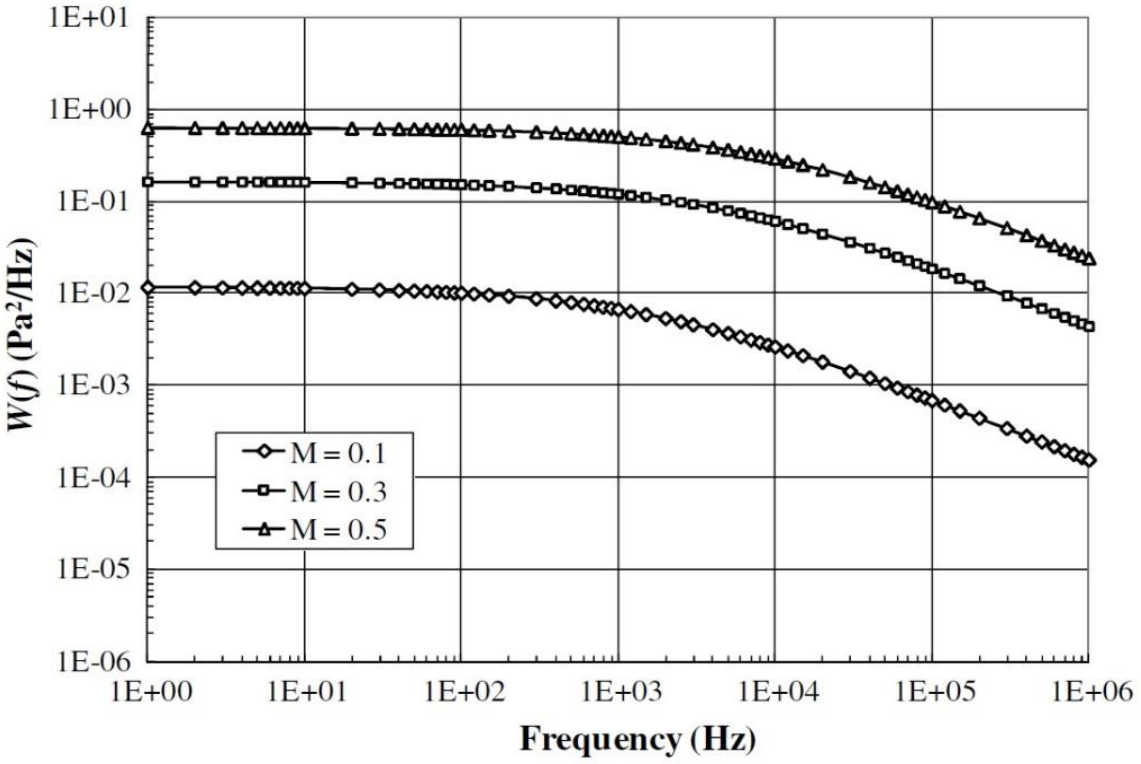

Fig. 4.9: Efimtsov 1 experimental pressure spectral density at M = 0.1, 0.3 and 0.5 [43]

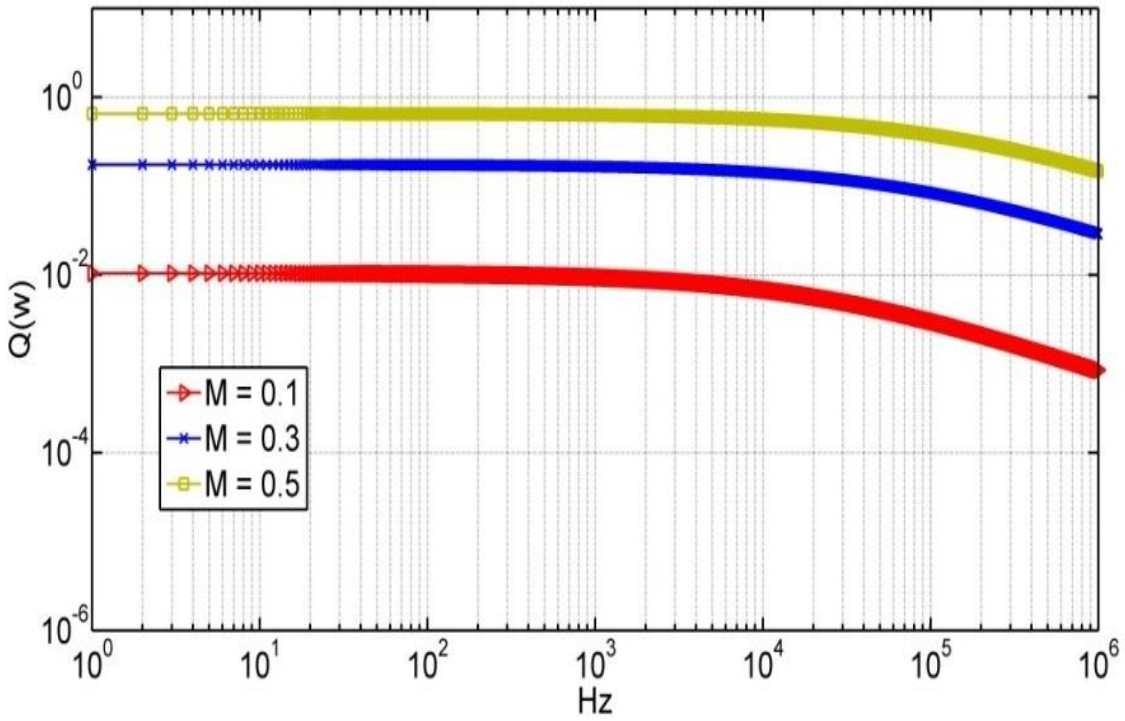

Fig. 4.10.Efimtsov 1 experimental pressure spectral density at M = 0.1, 0.3 and 0.5 (Present work)

4.3.3. STRUCTURAL RESPONSE

As discussed earlier the structural response of the plate due to TBL can be obtained by the approach used by Hambric *et. al.* [48] and Rocha *et. al.* [50] which is shown.

$$G_{uu}(y_i, y_j, \omega) \cong \sum_{\mu=1}^{N} \sum_{\nu=1}^{N} H_{u,F}^{*}(y_i|x_\mu, \omega) \Phi_{pp}(x_\mu, x_\nu, \omega) H_{u,F}(y_j|x_\nu, \omega) A_\mu A_\nu \quad (4.1)$$

Where, A_μ and A_ν are the area of the elements. As the number of elements increase, the area of the element decrease. This leads to accuracy of the work. The structural response of the plate with all four sides clamped (CCCC) for flow velocity 44.7 m/s is estimated. Initially in this work 60 x 6 and 30 x 21 mesh division are considered and compared with the numerical result published by Hambric [48], shown in Fig.. 4.11. It is observed that the accuracy is more in case of 30 x 21 meshing than 60 x 6. As the finer meshing demands higher computational facility and more time, 61 x 7 no. of elements are considered for all further analysis due to unavailability better computational facility.

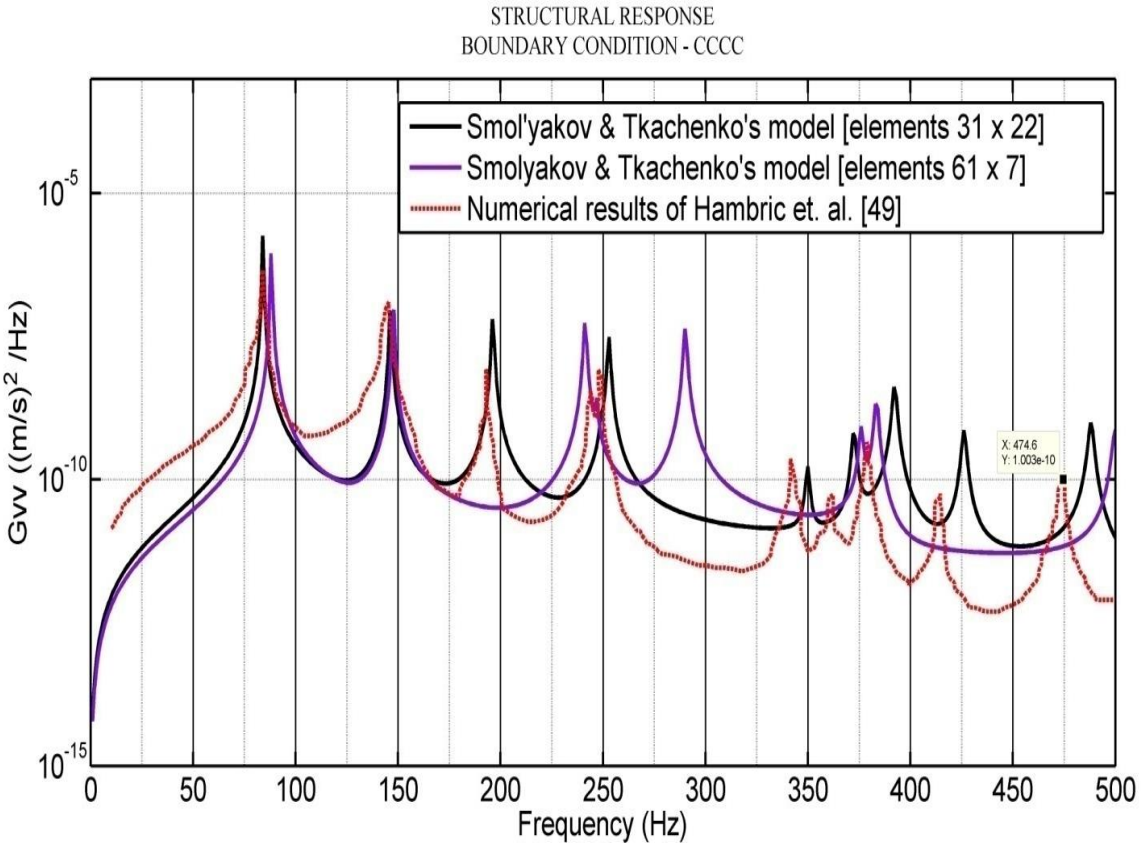

Fig. 4.11: Comparison of results with Hambric *et. al.* [48]

In the next stage of the work, the velocity spectrums of plate for different Mach number are compared. Three different PSD models are applied to obtain the velocity spectrum. The comparisons are shown in the Fig. 4.12 (a), (b) and (c).

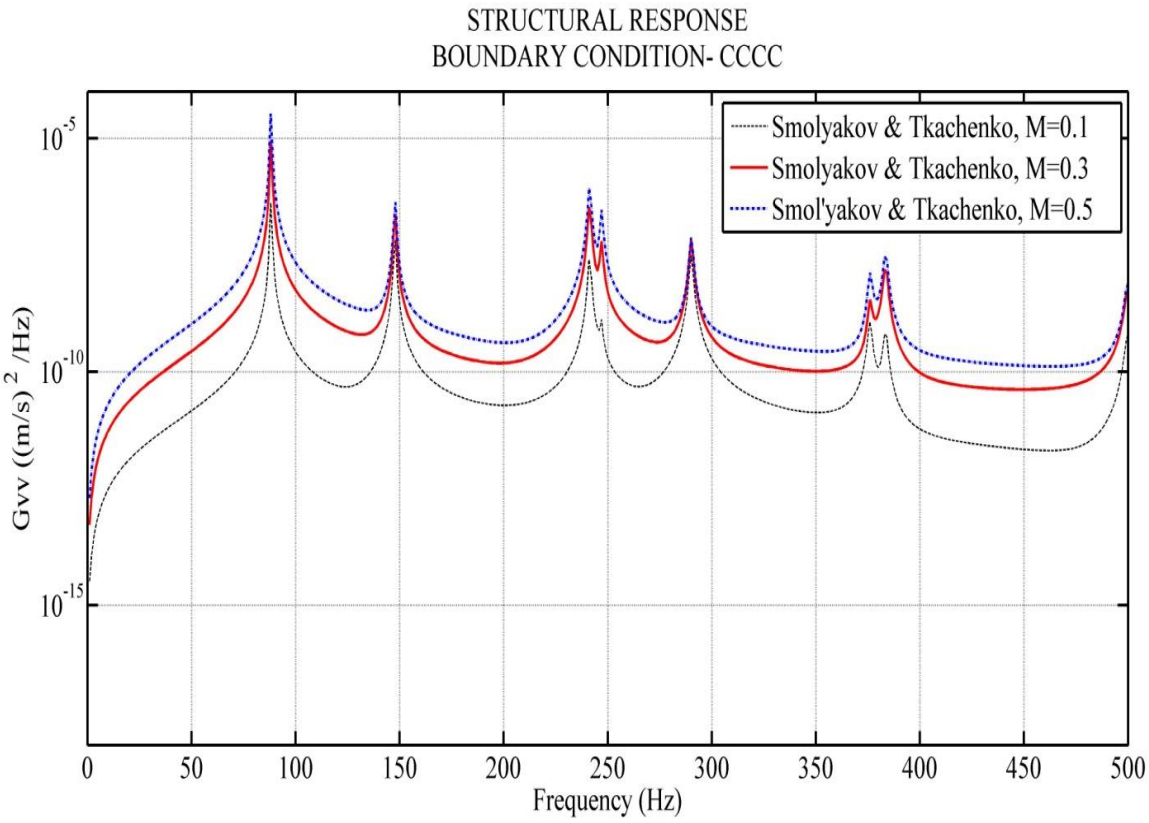

Fig. 4.12(a): Variation in structural response with Mach numbers (Present work)

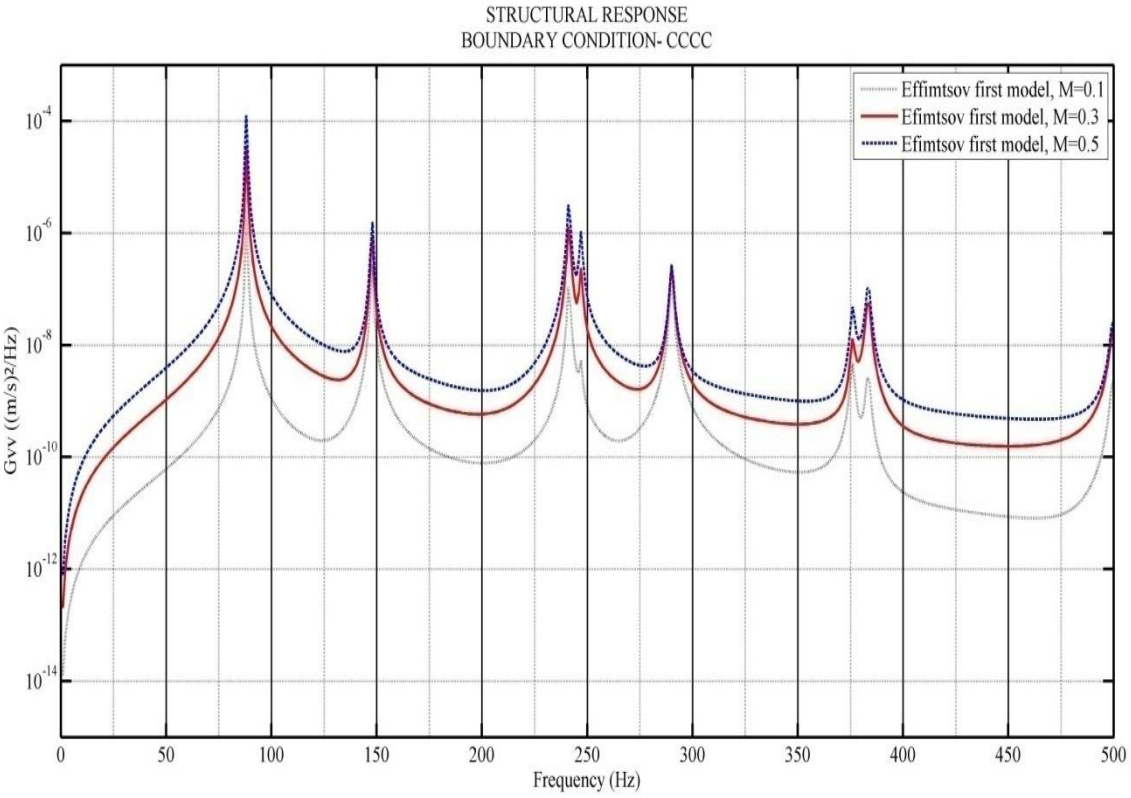

Fig. 4.12(b): Variation in structural response with Mach numbers (Present work)

It is evident from the Fig. 4.12 (a), (b) and (c) that the structural responses depend on flow Mach number. Fig. 4.12(a) shows the comparisons of structural response by using Smolyakov and Tkachenko's model [58] for different Mach numbers. The plots clearly indicate that the velocity spectrum is highest for Mach number 0.5 and lowest for Mach number 0.1. As per Smolyakov and Tkachenko's [58] model the single-point wall-pressure spectrum is proportional to $U_0^{3.5}$, which is the major reason of this variation of velocity spectrum.

The comparison of Goody's model [21] and Efimtsov's first model [15] shows that the experimental power spectral density of Goody's model [21] is in the lower side than Efimtsov's first model [15] at low frequency range, which is also reported by Niloufar [31]. In this present work the velocity spectrum shows the same trend at low frequency range (0-500 Hz). Goody's model [21] accounts spectral level decay as ω^{-5} where Smolyakov and Tkachenko's model [58] and Efimtsov's model [15] decay as $\omega^{-7/3}$ and $\omega^{-2/3}$ respectively. That is the major reason that the velocity spectrum is lowest for Goody' model [21] and highest for Efimtsov [15] and Smolyakov and Tkachenko [58] in the low-mid frequency range.

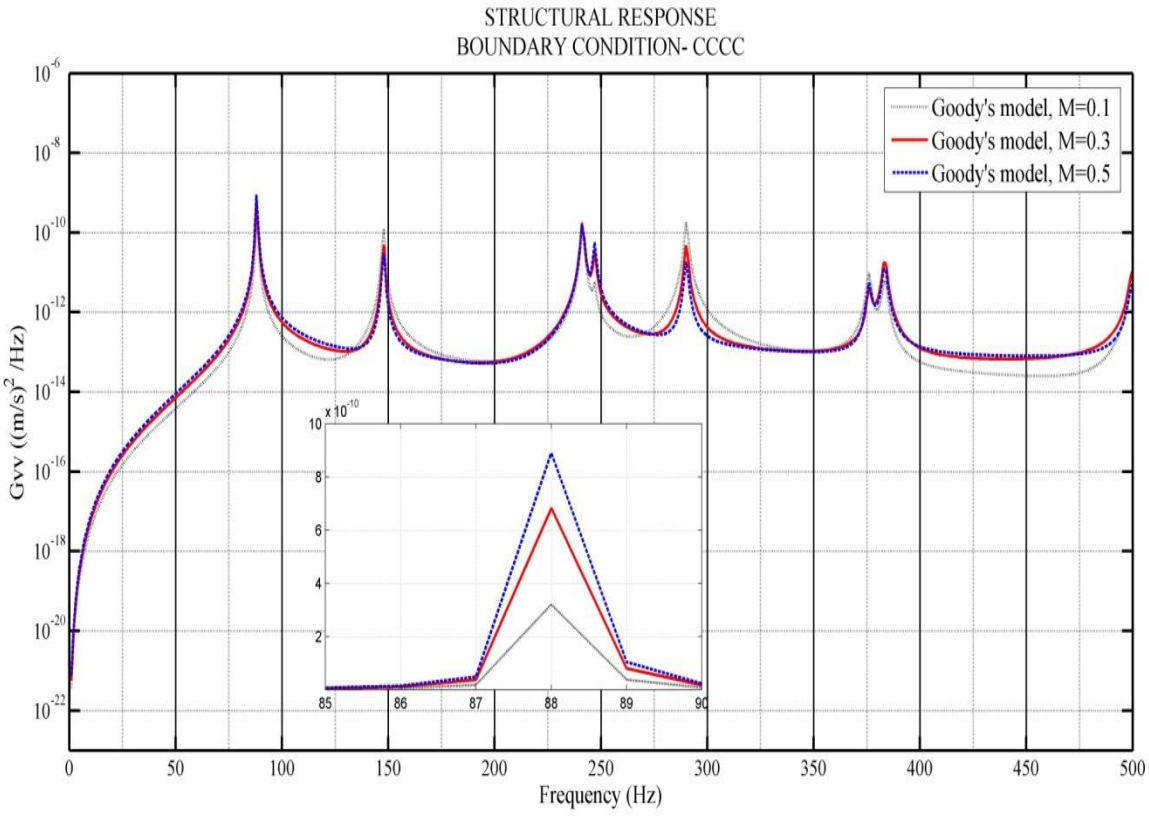

Fig. 4.12(c): Variation in structural response with Mach numbers (Present work)

Comparing with the other two models the effect of Mach number on Goody's model is very less but it follows the same pattern. That means the velocity spectrum increases with the increase in Mach number which is shown in Fig.: 4.12(c).

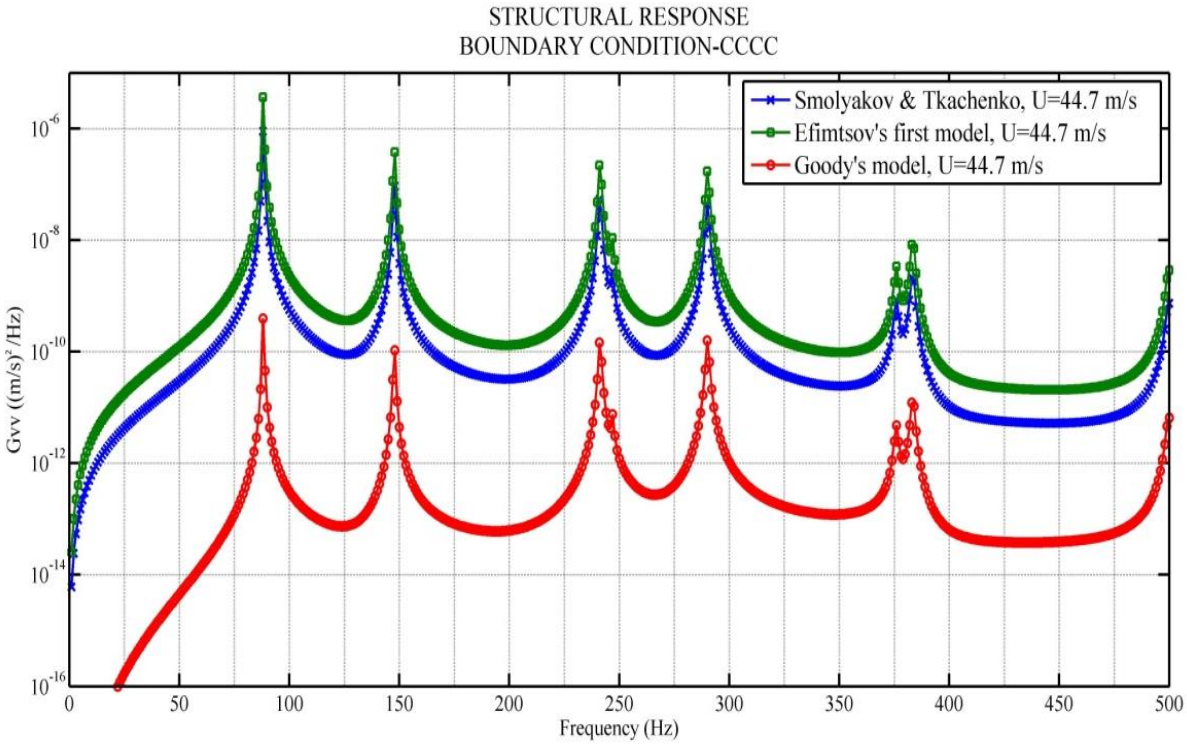

Fig. 4.13: Structural response of an all edges clamped flat plate for U = 44.7 m/sec (Present work)

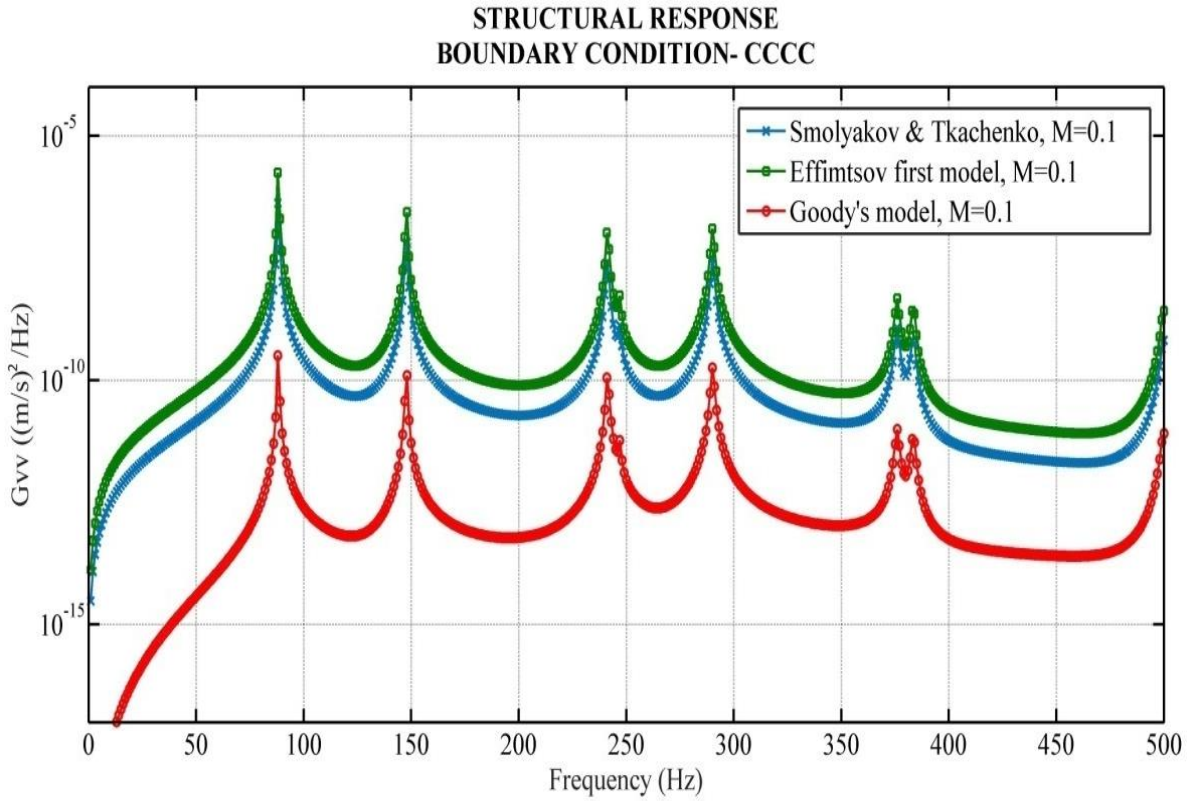

Fig. 4.14: Structural response of an all edges clamped flat plate for M = 0.1 (Present work)

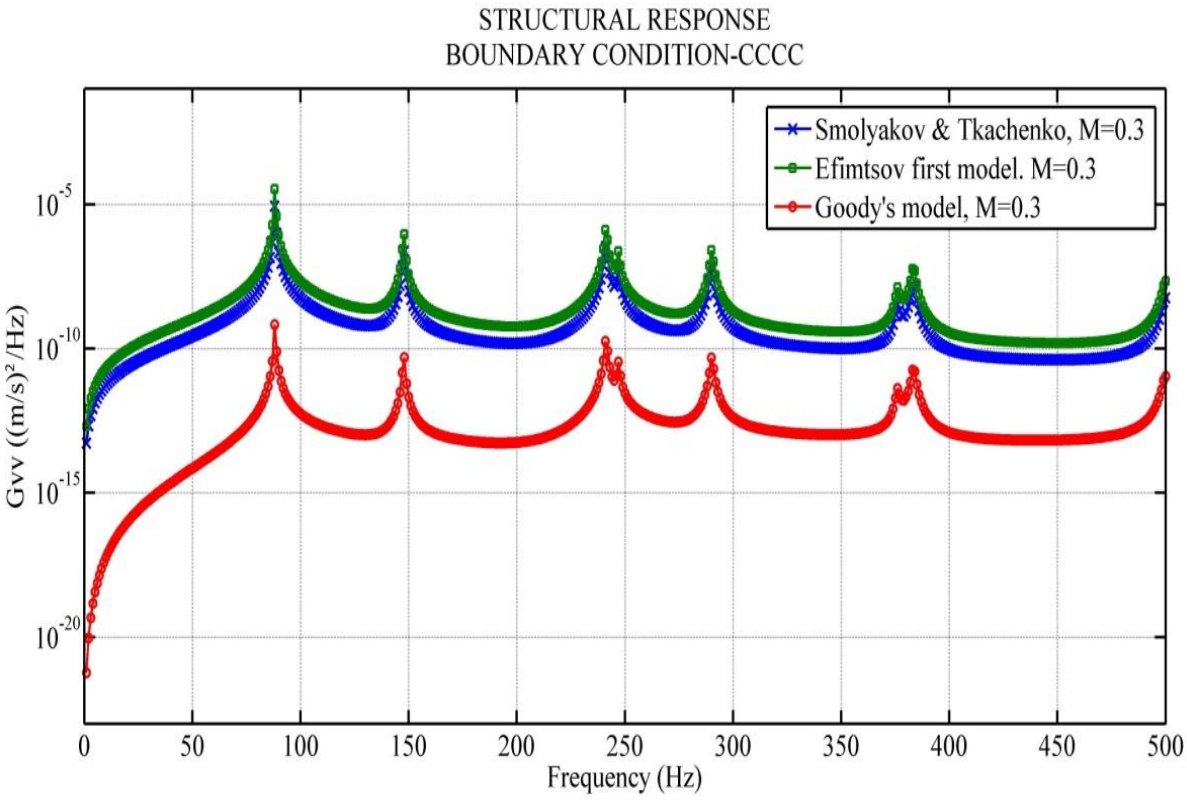

Fig. 4.15: Structural response of an all edges clamped flat plate for M = 0.3 (Present work)

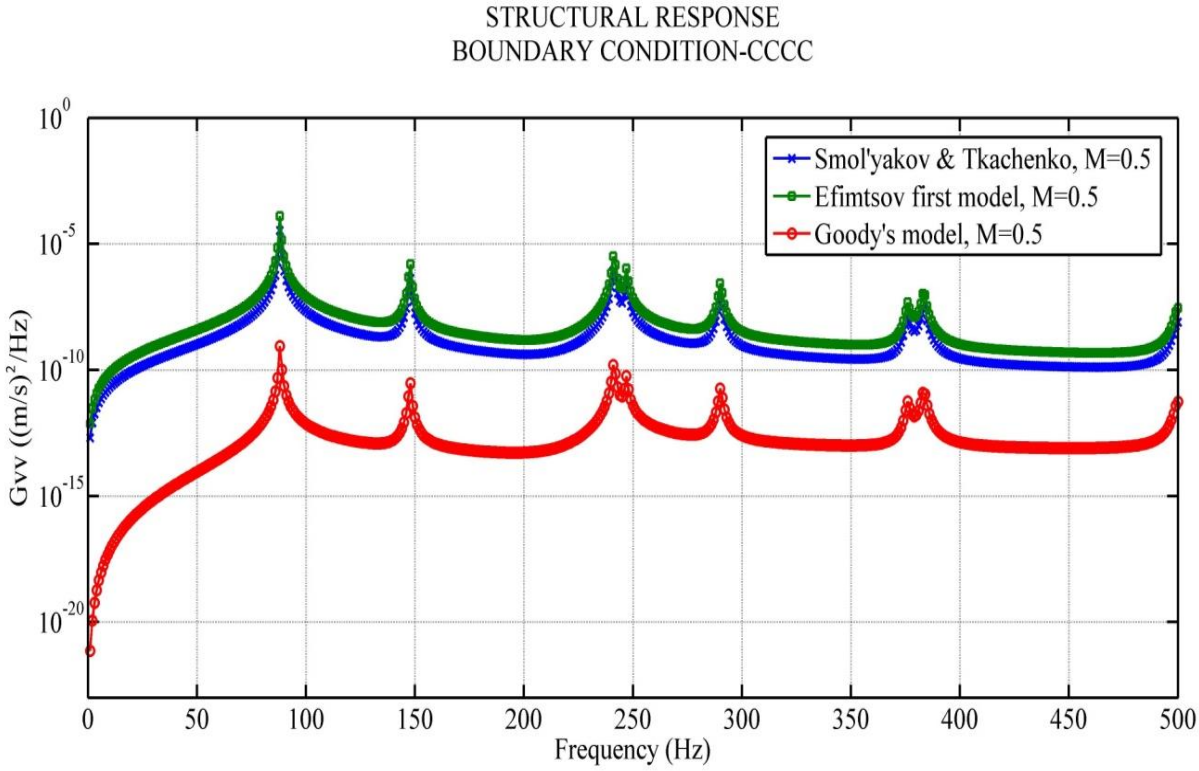

Fig. 4.16: Structural response of an all edges clamped flat plate for M = 0.5 (Present work)

In this part of the work the structural response of a cantilever plate is estimated in terms of velocity spectrum. To obtain the response of the plate different TBL models are applied. Fig. 4.17, 4.18 and 4.19 shows the velocity spectrum for Mach number 0.1, 0.3 and 0.5 respectively.

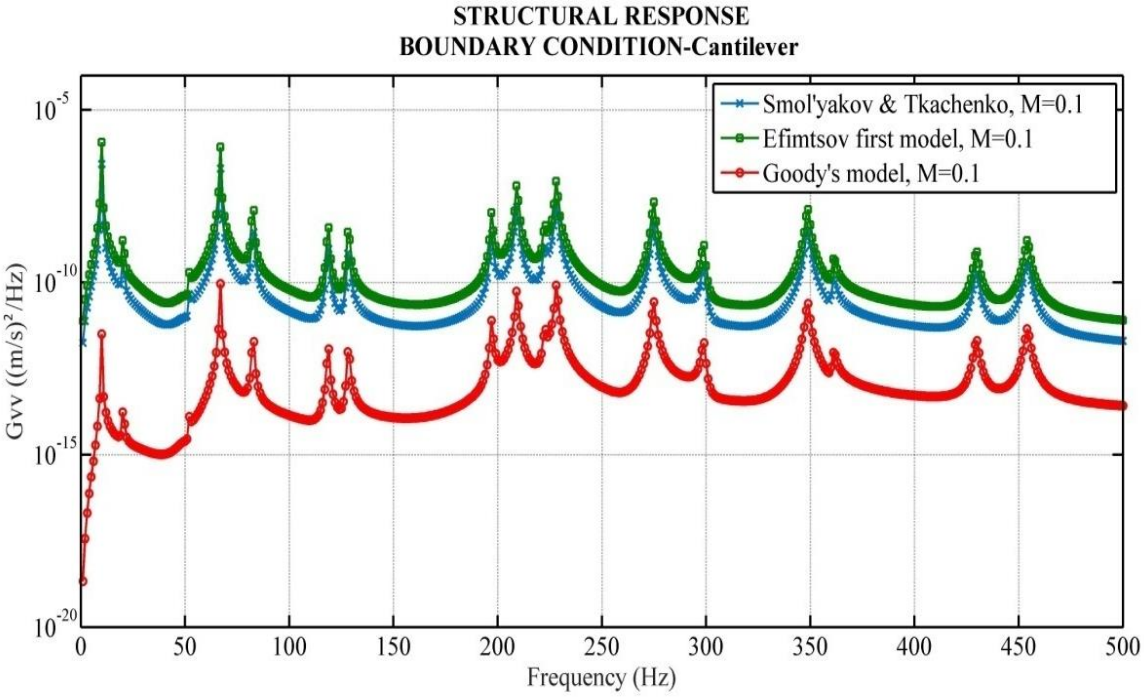

Fig. 4.17: Structural response of a cantilever flat plate for M = 0.1 (Present work)

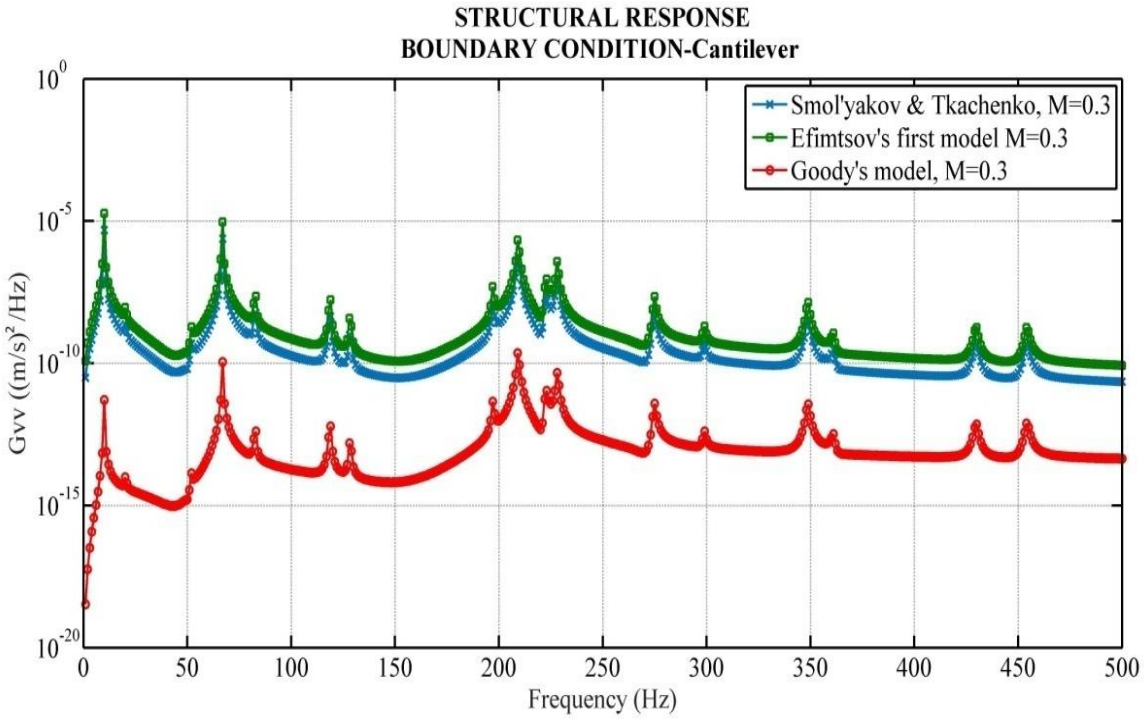

Fig. 4.18: Structural response of a cantilever flat plate for M = 0.3 (Present work)

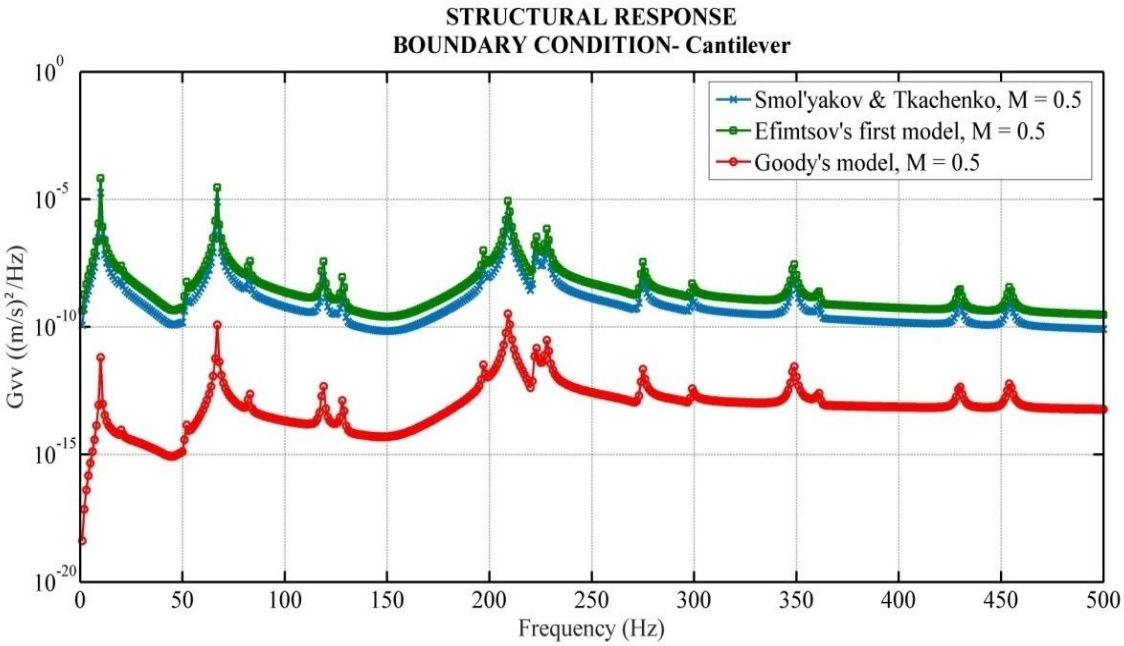

Fig. 4.19: Structural response of a cantilever flat plate for M = 0.5 (Present work)

From the structural response of the cantilever plate it is shown that the velocity spectrum increases with Mach number, which is similar to the CCCC condition. Secondly, the Goody's model under predict the structural response where Efimtsov's first model is in the higher end. By comparing the structural response of all edges clamped plate to the cantilever plate, it is observed that numbers of frequencies is higher for cantilever, because cantilever plate is more flexible.

In the next phase of work the structural response of a simply supported plate is estimated by applying three different PSD models for different Mach number.

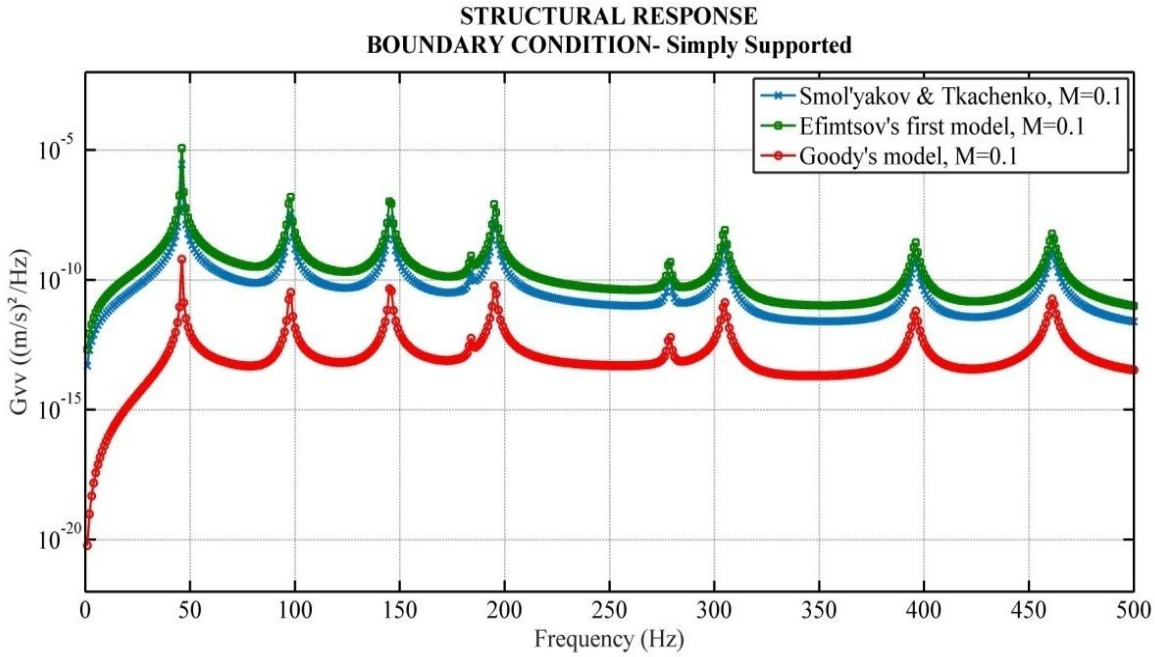

Fig. 4.20: Structural response of an all edges simply supported flat plate for M = 0.1 (Present work)

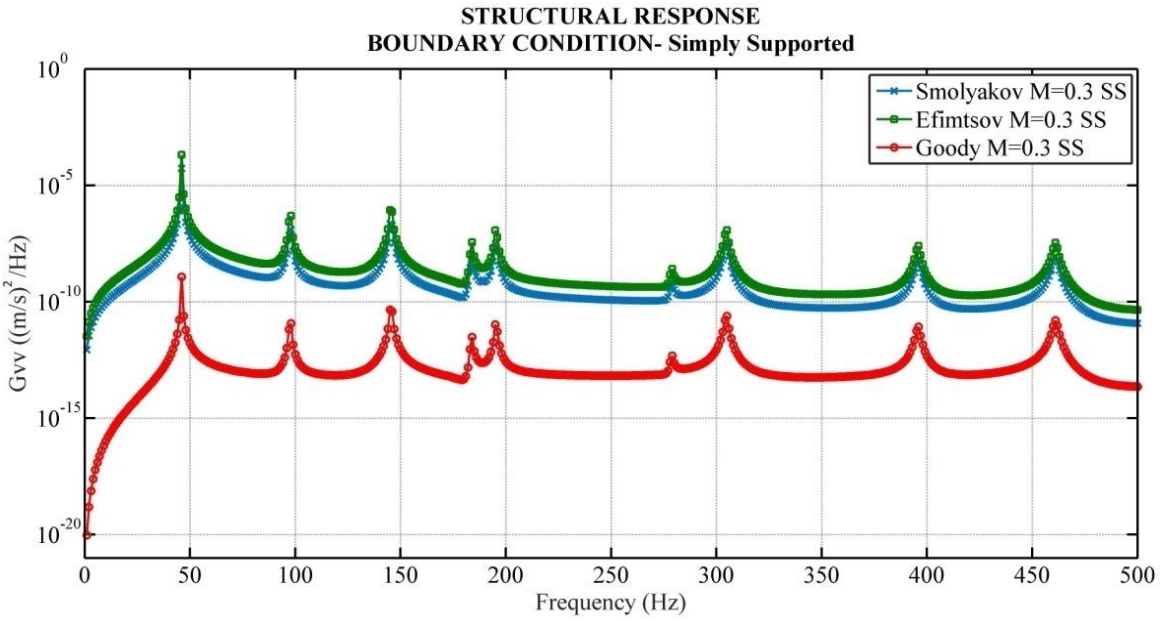

Fig. 4.21: Structural response of an all edges simply supported flat plate for M = 0.3 (Present work)

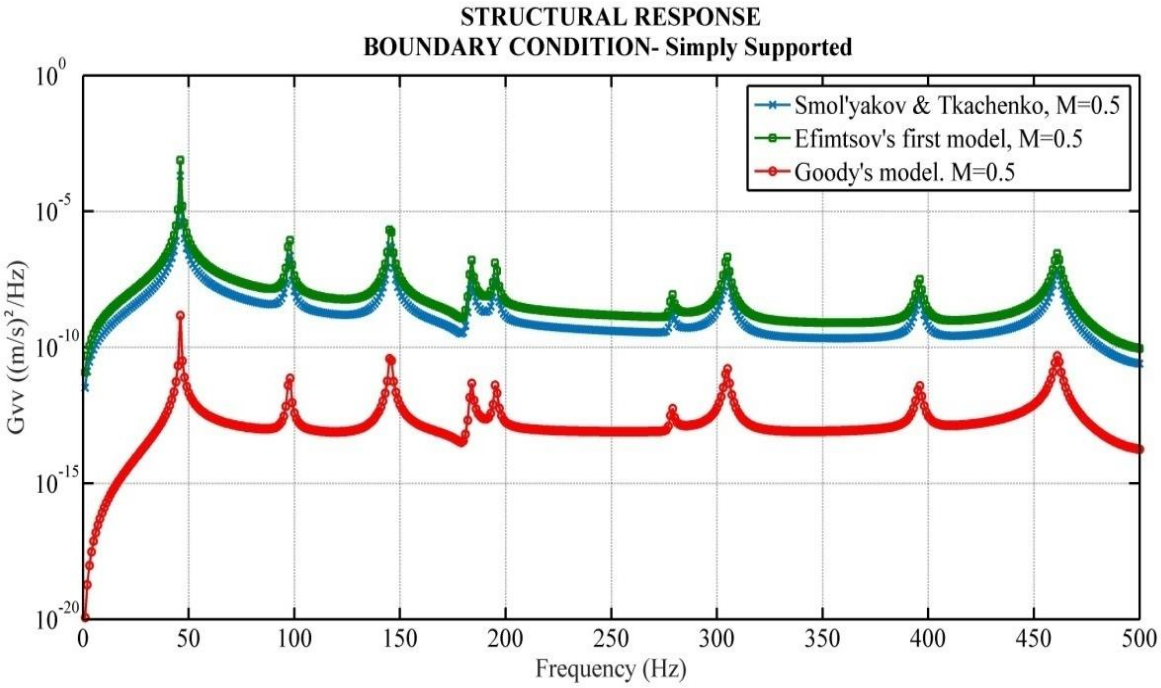

Fig. 4.22: Structural response of an all edges simply supported flat plate for M = 0.5 (Present work)

Important observation from the structural response of a simply supported flat plate

1. The response of the simply supported plate is higher than all edges clamped plate; just because of all edges clamped plate is stiffer than simply supported.
2. It also shows the similar trend with the variation in the Mach number. The velocity spectrum increases with increase in Mach number.
3. Here also Goody's model is in the lower end where Efimtsov's first model is in the higher end.

Chapter – 5

Conclusion and Future Scope

5.1. SUMMARY AND CONCLUSION

5.1.1. SUMMARY

The purpose of this project was to estimate the structural response by varying the flow parameter and structural parameter by using various single-point wall-pressure models. For this purpose, three single-point wall-pressure models are studied for different Mach number. In this work also the various finite elements parameters such as number of elements, area of the elements etc. which affect the structural response are also examined.

5.1.2. CONCLUSION

1. A detailed review of literatures is carried out and major gaps in the earlier works are highlighted. It is seen from the previous works either only TBL models are considered or it deals with the structural response of the plate subjected to TBL excitation. On this basis the objective of the presented work is founded. The effect of flow parameter on flow spectrum and also on velocity spectrum is observed for different boundary condition.
2. Single-point wall-pressure spectrum is estimated by using three different semi-empirical models in MATLAB environment. The semi-empirical models are Smolyakov and Tkachenko's model, Efimtsov's first model, Goody's model. A coherence function is used with the average autospectral density to get the cross-power spectral density.
3. Free vibration analysis of rectangular plate with three different boundary conditions is performed using APDL. A convergence study also performed to understand how the accuracy of result is depending on meshing. As an end results of this stage natural frequency and mode shape data is obtained.
4. The frequency, mode shape data obtained from free vibration analysis is used in MATLAB to estimate the frequency response function (FRF). For this a MATLAB code is developed.
5. In the last stage, the structural response is measured in terms of velocity spectrum. To obtain the final result, FRF is coupled with cross-power spectral density. Due to the limitation in the computational facility, structural response is measured for low to medium frequency range (0-500 Hz) where the flow spectrum is estimated for (0-10^5 Hz).

Some of the important observations from the obtained results are cited below:

1. From the previous discussion in the Chapter-4 it can be concluded that the single-point wall-pressure spectrum or the experimental power spectral density increases with the increase in Mach number. As a result, the velocity spectrums also follow the same trends. It can be clearly be seen that the

spectral density obtained by using Smolyakov and Tkacheko's model [58] and first model of Efimtsov [15] are proportional to free stream velocity, which is the major reason f this trends. In case of Goody's model [21], the same variation of spectral density with the Mach number can be observed but this variation is negligible. That means the effect of free stream velocity on the spectral density is very small for Goody's model [21].

2. At the low to mid frequency range (0-500 Hz) the velocity spectrum is in the lower side for Goody's model [21] and Efimtsov [15] is in the highest end. The decaying in spectral level as ω^{-5} is introduced by Goody [21] to get better agreement with the experimental results. Hambric *et. al.* [48] compared the Smolyakov and Tkachenko's model [58] with an experimental result and also obtained a better agreement. By considering the Hambric's [48] work as a base line it can be concluded that the Goody's model [21] under predict the structural responses where Efimtsov's model [15] over predicts in the low-mid frequency regime.
3. The major concern is the number of elements in the numerical modelling because it's effect the accuracy of the work. As discussed earlier with the increase in number of elements the computational times increase demanding better computational facility.
4. From the view of boundary conditions, it can be concluded that the more number of picks is observed in case of cantilever than the clamped and simply supported conditions which is quite obvious.

5.2. FUTURE SCOPE OF WORK

Although an attempt is made in the present work to understand the structure response subjected TBL flow over flat plate, there are immense scopes to take this work into the next level.

(i) This work can be further extended to the estimation of sound pressure level (SPL).

(ii) If better computational facility is available than the effect of finer discretization of the element on the structural response can be performed.

(iii) This project can be further extended to the effect in structural response and SPL due to change in the dimension, thickness and curvature of the plate.

(iv) In the next level investigation, composite plate, with stiffener or multi-panel and ribbed plate can be considered in order to estimate structural vibration and radiated noise pressure.

(v) Considering a real life structural form representing a vehicle structure cab be analysed for estimating vibration and sound pressure level.

REFERENCES

[1] Robert H. Kraichnan, Acoustics Laboratory, Columbia University, New York 27, New York, "Pressure Fluctuations in Turbulent Flow Over a Flat Plate", Journal of the Acoustical Society of America, Vol. 28, No. 3, May 1956, pp. 378–390.Doi:10.1121/1.1908336.

[2] Lilley, G. M., and Hodgson, T. H., "On Surface Pressure Fluctuations in Turbulent Boundary Layers," Advisory Group for Aeronautical Research and Development Rept. 276, April 1960.

[3] Willmarth, W. W., and Wooldridge, C. E., "Measurements of the Fluctuating Pressure at the Wall Beneath a Thick Turbulent Boundary Layer," Journal of Fluid Mechanics, Vol. 14, No. 2, Oct. 1962, pp. 187–209.Doi: 10.1017/S0022112062001160

[4] G.M.Corcos, Resolution of Pressure in Turbulence, The Journal of Acoustic society of America, 1963.

[5] G.M.Corcos, The Resolution of Turbulent Pressure at the wall of a Boundary layer, J.SoundVib. (1967).

[6] John E. Ffowcs Williams, "Suface-pressure fluctuations induced by boundary-layer flow at finite Mach number", J. Fluid Mech., (1965)

[7] M.K.Bull. Department of Mechanical Engineering, University of Adelaide, South Australia, "Wall-pressure fluctuations associated with subsonic turbulent boundary layer flow", (1967) & "Wall-Pressure Fluctuations beneath Turbulent Boundary Layers: Some Reflections on Forty Years of Research," Journal of Sound and Vibration, Vol. 190, No. 3, 1996, pp. 299–315.Doi:10.1006/jsvi.1996.0066.

[8] Lowson, M.V., "Predictionn of Boundary Layer Pressure Fluctuation", U.S. Air Force Dyanamics Lab. TR 67-167, April 1968.

[9] Blake, W. K., "Turbulent Boundary-Layer Wall- Pressure Fluctuations on Smooth and Rough Walls",Journal of Fluid Mechanics, Vol.44, No. 4, 1970, pp. 637-660.

[10] Schewe, G., "On the Structure and Resolution of Wall-Pressure Fluctuations Associated with Turbulent Boundary Layer Flow",Journal of Fluid Mechanics, Vol. 134, 1983, pp. 311-328. DOI:10.1017/S0022112083003389.

[11] Lauchele, G.C., and Daniels, M. A., "Wall-Pressure Fluctuation in Turbulent Pipe Flow", Physics of Fluids, Vol.30, No.10, Oct.1987, pp. 3019-3024.

[12] Farabee, T. M., and Casarella, M. J., "Spectral Features ofWall Pressure Fluctuations Beneath Turbulent Boundary Layers," Physics of Fluids, A, Vol. 3, No. 10, Oct. 1991, pp. 2410–2420.Doi:10.1063/1.858179.

[13] Lueptow, R. M., "Transducer Resolution and the Turbulent Wall Pressure Spectrum", Journal of the Acoustical Society of America, Vol.97, No.1, Jan.1995, pp.370-378.

[14] Robertson, J. E., “Prediction of In-Flight Fluctuating Pressure Environments Including Protuberance Induced Flow,” NASA CR- 119947, March 1971.

[15] Efimtsov, B. M., “Characteristics of the Field of Turbulent Wall Pressure Fluctuations at Large Reynolds Numbers,” Soviet Physics Acoustics, Vol. 28, No. 4, July–Aug. 1982, pp. 289–292.

[16] Efimtsov, B. M., Kozlov, N. M., Kravchenko, S. V., and Andersson, A.O., “Wall Pressure-Fluctuation Spectra at Small Forward-Facing Steps,” AIAA Paper 1999-1964, 1999.

[17] Howe, M.S.,”On the Structure of the the Turbulent Boundary-Layer Wall Pressure Spectrum in the Vicinity of the Acoustic Wavenumber,” Proceeeding of the the Royal Society of London A, Vol.412, 1987, pp.389-401. DOI:10.1098/rspa.1987.0093.

[18] Chase, D. M., “Modeling the Wavevector-Frequency Spectrum of Turbulent Boundary Layer Wall Pressure,” Journal of Sound and Vibration, Vol. 70, No. 1, 1980, pp. 29–67.Doi:10.1016/0022-460X(80)90553-2.

[19] Smol’yakov, A. V., “Calculation of the Spectra of Pseudosound Wall-Pressure Fluctuations in Turbulent Boundary Layers,” Acoustical Physics, Vol. 46, No. 3, 2000, pp. 342–347.Doi:10.1134/1.29890.

[20] Smol’yakov, A. V., and Tkachenko, V. M., “Model of a Field of Pseudosonic Turbulent Wall Pressures and Experimental Data,” Soviet Physics- Acoustics, Vol. 37, No. 6, 1991, pp. 627–631.

[21] Goody, M. C., “Empirical Spectral Model of Surface Pressure Fluctuations,” AIAA Journal, Vol. 42, No. 9, Sept. 2004, pp. 1788–1794.Doi:10.2514/1.9433. Goody, M. C., “Unsteady Pressures on the Surface of a Ship Hull,” Proceedings of IMECE2007, 2007 ASME International Mechanical Engineering Congress and Exposition, Seattle WA, American Soc. of Mechanical Engineers Paper 2007-41673, Fairfield, NJ, Nov. 2007.

[22] Rackl, R., and Weston, A., “Modeling of Turbulent Boundary Layer Surface Pressure Fluctuation Auto and Cross Spectra- Verification and Adjustments Based on TU-144LL Data,” NASA CR-2005-21398, Dec. 2005.

[23] Yannick Rozenberg, Gilles Robert, Stephane Moreau, “Wall-pressure spectral model including the adverse pressure gradient,” AIAA Journal, American Institute of Aeronautics and Astronautics, Vol. 50 (10), pp. 2168-2179, 2012.

[24] G. M. Corcos, Resolution of Pressure in Turbulence, The Journal of Acoustic society of America, 1963. G. M. Corcos, The Resolution of Turbulent Pressure at the wall of a Boundary layer, J. Sound Vib., 1967.

[25] Mellen R.H. (1990), “On modeling convective turbulence”. Journal of the Acoustical Society of America.

[26] R.H. Mellen, “Wave-vector filter analysis of turbulent flow”, J. Acoust. Soc. Am. 95(3), 3885-3899 (1994). Doi:10.1121/1.408556

[27] Philippe R. Spalart, “Direct simulation of a turbulent boundary layer up to $R_\theta = 1410$,” J. Fluid Mech., vol. 187, pp. 61-98, 1988.

[28] Wang, M., "Dynamic Wall Modeling for LES of Complex Turbulent Flows, "Annual Research Briefs, CTR, Stanford University, pp. 241–250, 2000.

[29] Xiaohua Wu and ParvizMoin, “Direct numerical simulation of turbulence in a nominally zero-pressure-gradient flat-plate boundary layer.” J. Fluid Mech., vol. 630, pp. 5-41, 2009.

[30] DanielJuvé, Marion Berton and EdouardSalzeSpectral Properties of Wall-Pressure Fluctuations and Their Estimation from Computational Fluid Dynamics, Springer International Publishing Switzerland 2015

[31] Niloufar Mahmoudnejad, “Numerical simulation of wall-pressure fluctuations due to turbulent boundary layer,” PhD Thesis, Department of Aerospace Engineering, Wichita State University, 2011.

[32] Zeno Belligoli, Henrich Luedeke, “DNS of Simple Verification Test Cases Using OpenFOAM”, Report of the Institute of Aerodynamics and Flow Technology, 2014.

[33] M. K. Bull and A. S. W. Thomas, “High frequency wall pressure fluctuations in turbulent boundary layers,” Physics of Fluids, vol. 19, pp. 597 – 599, 1976

[34] R. Emmerling, G. Meier and A. Dinkelacker, “Investigation of the instantaneous structure of the wall pressure under a turbulent boundary layer flow,” AGARD Conference Proceedings No. 131, on Noise Mechanisms, 24 – 1, 1973.

[35] M. K. Bull and Th. Langeheinken, “On the wall pressure field in turbulent pipe flow,” Mitteilungenaus dem max-planck-Institut fur Stromungsforchung, Gottingen, Nr. 73, 1981.

[36] Nan HU, Malte Misol, “Effects of riblet surface on boundary-layer-induced surface pressure fluctuations and surface vibration,” DAGA 2015 Nurnberg.

[37] W. W. WILLMARTH AND C. S. YANG, Wall-pressure fluctuations beneath turbulent boundary layers on a flat plate and a cylinder, J. Fluid Mech. (1970)

[38] W. V. BHAT, Flight test measurement of exterior turbulent boundary layer pressure fluctuations on boeing model 737 airplane, J. Sound Vib. (1971)

[39] J. F. WILBY AND F. L. GLOYNA, Vibration measurements of an airplane fuselagestructure due to turbulent boundary layer excitation, Journal of Sound and Vibration (1972)

[40] J.Sulc, J.Hofr and L.Benda,”Exterior noise on the fuselage of light propeller driven aircraft in flight”, Journal of Sound and Vibration, Vol-84, 1982.

[41] G.Cousin, “Sound from TBL-induced vibrations”, American Institute of Aeronautics and Astronautics, Inc., 1998

[42] Lee and Sung, Characteristics of wall pressure fluctuation in separated and reattaching flow over a backward-facing step, Experiment in fluid, 2001

[43] T. S. Moller, “Turbulent boundary layer models for acoustic analysis,” PhD Thesis, Department of Aerospace Engineering, Wichita State University, 2011.

[44] TANG Weilin, “Noise radiation of an elastic plate excited by TBL pressure fluctuation”, Harbin Shipbuilding Engineering Institute, 1991.

[45] S. Hambric, Y. F. Hwang, “Vibrations of flat plates excited by low Mach number turbulent boundary layers.” The 29th International Congressand Exhibition on Noise Control Engineering 27 – 30 August 2000, Nice, France.

[46] Pierre Hardy, Louis Jezequel, Mohammed Ichchou and Yves Jacques, “ Turbulent boundary layer induced vibration up to high frequencies by means of local energy methods, The Journal of Acoustical Society of America, 2002

[47] S.Finnveden, F.Birgersson, U.Ross and T.Kremer, “A model of wall pressure correlation for prediction of turbulence-induced vibration”, Journal of Fluid and Structure, 2005.

[48] S. A. Hambric, Y. F. Hwang, W. K. Bonness, “Vibration of plates with clamped and free edges excited by low-speed turbulent boundary layer flow,” Journal of Fluids and Structures, vol. 19, pp. 93 – 110, 2004.

[49] Yang. Z, Voke, P.R., 2001. Large-eddy simulation of boundary-layer separation and transition at a change of surface curvature. Journal of Fluid Mechanics

[50] Rocha *et. al.*, “Turbulent Boundary Layer Noise and Vibration of a Multi-panel walled acoustic enclosure:, Canadian Acoustics, 9-vol.38, No. 4 (2010).

[51] LI Zuhui, CHEN Meixia, “Numerical method for calculating sound radiation characteristics of plate structure excited by turbulent boundary layer”, School of Naval Architecture and Ocean Engineering, University of Science and Technology, Wuhan 430074, Chaina. 2017

[52] Alexander Klabes et al, Aircraft Fuselage Vibration Excitation by Turbulent Boundary Layer Flow in Cruise

[53] LI Zuhui, CHEN Meixia, “Numerical method for calculating sound radiation characteristics of plate structure excited by turbulent boundary layer”, School of Naval Architecture and Ocean Engineering, University of Science and Technology, Wuhan 430074, Chaina. 2017

[54] Micah R Shepherd and Stephen A Hambric, “Structural-acoustic optimization of a pressurized, ribbed panel”, Proceedings of Meetings on Acoustics 22, 065002 (2014); 10.1121/2.0000014.

[55] Bilong Liu, Hao Zhang, ZhongchangQian, Daoqing Chang, Qun Yan, Wenchao Huang, Key Laboratory of Noise and Vibration Research, Institute of Acoustics, Chinese Academy of Sciences, PR China, Key Laboratory of Aeroacoustics and Dynamics, Aircraft Strength Research Institute, 710065 Xian, PR China, “Influence of stiffeners on plate vibration and radiated noise excited by turbulent boundary layer”, Applied Acoustics 80 (2014) 28-35

[56] F.X.Xin and T.J.Lu, “Effects of mean flow on transmission loss of orthogonally rib-stiffened aeroelastic plates”, The Journal of the Acoustical Society of America 133, 3909 (2013); doi:10.1121/1.4802644.

[57] Vivien Denis *et. al.*, “Prediction of flow induced sound and vibration of periodically stiffened plates”, HAL ID: hal-00744516, 2018

[58] Smolyakov, A. V., and Tkachenko, V. M., “Model of a Field of Pseudosonic Turbulent Wall Pressures and Experimental Data,” Soviet Physics- Acoustics, Vol. 37, No. 6, pp. 627–631, 1991.

[59] L.J Peltier, S.A. Hambric, “Estimating turbulent-boundary-layer wall-pressure spectra from CFD RANS solutions”, Journal of Fluid and Structure 23 (2007) 920-937.

[60] Review of TBL Models for Acoustic Analysis, Teresa S. Miller, Bombardier Learjet, Wichita, Kansas 67277 and Judith M. Gallman and Mark J. Meller, Sprite Aerosystems, Inc., Wichita, Kansas 67278-0008; DOI:10.2514/1.C031

[61] Dowell, E. H. (1975). Aeroelasticity of Plates and Shells (Noordhoff, Groningen, The Netherlands).

[62] Saikat Sarkar, Biplab Ranjan Adhikary, Partha Bhattacharya, “Turbulent Boundary Layer Excitation and Vibration Reduction Techniques for past 60 Years: a Review”, (20180349) STRUCTURAL ENGINEERING CONVENTION-2018

[63] White, F.M. 1991. Viscous fluid flow. McGraw-Hill, New-York, NY.